REPUBLIQUE ALGERIENNE DEMOCRATIQUE ET POPULAIRE
Ministère de l'Enseignement Supérieur et de la Recherche Scientifique

N° Série :……/2022

Université Kasdi Merbah Ouargla

Faculté des Hydrocarbures, Energies Renouvelables et Science de la Terre et de l'Univers

Département de Production des Hydrocarbures

MÉMOIRE

Pour obtenir le Diplôme de Master

Option : Production Professionnelle

Présenté Par :

BOUTERAA Nour Elislam, BOUCHEFA Abderraouf, DJERRAYA Amor

-THÈME-

Guelta North 3D dynamic simulation model update and development option. Ohanet region Illizi basin, Algeria

Soutenue le : 07 / 06 / 2022 devant la commission d'examen

Jury :

Président :	Mr. KADRI Ahmed Yacine	MAA	Univ. Ouargla
Examinateur :	Mr. MAHSSOUEL Ammar	MCA	Univ. Ouargla
Rapporteur :	Mr. TOUIHRI Abdeldjebar	MCB	Univ. Ouargla
Co-encadreur :	Mr. ADJOU Zakaria	Doctorant	Univ. Ouargla

Année Universitaire 2021/2022

Acknowledge

First of all, we would like to thank ALLAH the merciful for giving us the strength, luck and patience to complete this modest work.

We express our gratitude to ***Mr. TOUAHRI Abdel Djebar*** *and* ***Mr. ADJOU Zakaria*** *for the confidence that has shown us by agreeing to follow this theme, his advice, his seriousness and his availability.*

We thank the review board for agreeing to review this work, for their support and constricting observations.

We also thank all the teachers, without forgetting the administrative team of the hydrocarbons production department of the University of Ouargla who participated directly or indirectly in our training during our course of study.

Finally, we thank our friends for having supported and encouraged us during all these years

Dedications

This study is wholeheartedly dedicated to my beloved Parents, who have been my source of inspiration and gave me strength with their prayers, guidance, and sacrifices when I thought about giving up.
To my brothers and sisters who shared their words of advice and encouragement through all these years.
Thank you everyone for introducing me to this mysterious domain.

Bouteraa Nour Elislam

Firstly, I'd like to express my sincere gratitude to my supportive parents for being my main source of inspiration, motivation & guidance.
From the bottom of my heart, I would like to say a big thank you to all my friends for their support and assistance in any way they could throughout the research project.
Last but not least, I want to thank my colleagues Djerraya Amor and Bouteraa Nour Elislam for their encouragement in everything related to this Project.

Bouchefa Abderraouf

First and foremost, I have to thank my parents for their Love, Support, Encouragement and caring over all these years, for being always there for me through thick and thin. Thank you both for giving me the strength to reach for the stars and chase my dreams.
I also don't want to forget ***Mr CHATTI Djamel*** *who provided assistance to me at the right time so he deserves a big thanks giving.*
I have to thank also Brothers and sisters for their support. encouragement and assistance. I Also would like to say a big thank for ***Mr. BERRIM Fahim*** *because he has a big part from this victory.*
At the end, of course My colleagues Raouf and Islam deserves a big thanksgiving.

Amor DJERRAYA

ملخص

يتكون هذا العمل من التطوير الفعال وتشغيل مكمن البترول لخزان **قلتة-شمال** الواقع في حوض إليزي ؛ من المهم أن يكون لديك نموذج خزان. يمكن أن يعمل نموذج المحاكاة العددية للمكمن كأداة مناسبة لإدارة المكمن للتنبؤ بالإنتاج من كل بئر في حقل به آبار متعددة. في نهاية هذا المشروع ، تُظهر النتائج بوضوح أن إنتاج الغاز قد انعكس وأكد أنه تقريبًا نفس النتيجة كما في الواقع. تم بناء النموذج الديناميكي خطوة بخطوة باستخدام برنامج **ECLIPSE black oil** في عام 2020.

الكلمات المفتاحية: النموذج الديناميكي ، المحاكاة، المكمن ، النتيجة.

Résumé

Ce travail consiste à développer et exploiter efficacement un réservoir pétrolier du réservoir Geulta-Nord situé dans le bassin d'Illizi ; il est important d'avoir un modèle de réservoir. Le modèle de simulation numérique de réservoir peut servir comme un outil approprié pour la gestion du réservoir afin de prédire la production de chaque puits dans un champ à plusieurs puits. À la fin de ce projet, les résultats montrent clairement que la production de gaz a reflété et confirmé être presque le même résultat en réel. Le modèle dynamique a été construit pas à pas avec le logiciel **ECLIPSE black oil** en 2020.

Mots clé : modèle dynamique, simulation, réservoir, résultat.

Abstract

This work consists of history matching update and development options of the dynamic model of Geulta-North Ordovician gas condensate reservoir located in the Illizi Basin (South Eastern part of the Algerian Sahara Desert), The dynamic model was built in ECLIPSE 100 black oil software in 2020. The different stages of the model construction were reported and described. The model consists of 98x77x50 cells grid up scaled from the static model which is composed of. The SCAL and PVT data were taken from the analogous similar reservoirs of nearby gas fields. The history matching of the model was obtained after several hundreds of realizations "run", carried out on uncertain parameters (local permeability, skin factor,) in the model. Four production scenarios over 50 years were simulated and evaluated to maximize recovery from this tight gas reservoir.

Key words: Dynamic model, simulation, reservoir, result.

Summary

List of figures

List of tables

Abbreviation list

Abbreviation	Nomenclature
PVT	Pressure volume temperature.
FVF	Formation Volume Factor.
STB	Stock tank barrel.
Cw	Water compressibility.
μw	Water Viscosity.
ρw	Water Density.
MW	Molecular Weight.
Pb	Bubble point.
GOR	Gas oil ratio.
p_{pc}	Pseudo-critical pressure.
T_{pc}	Pseudo-critical temperature.
Υ_g	Gas gravity.
MW_g	Molecular weight of the gas.
B_g	Gas volume factor.
PI	Productivity index.
IPR	Inflow performance relationship.
DST	Drill stem testing.
MBH	Miller Bronze Hazelbrook method.
IMFV	Incoming mass flux values.
OMFV	Outgoing mass flux values.
Ppr	Pseudo-reduced pressure.
Pp	Normalized pseudo-pressure function.
Q	Gas flow rate, scf/day.
Pwf	Flowing bottomhole pressure, psia.
GIIP	Gas initially in place.
OGIP	Original gas in place.
CPF	Centre of process & facilities.
LPG	Liquefied Petroleum Gas.
HP	Haigh pressure.
MP	Medium pressure.
LP	Low pressure.

NTG	Net to gross.
CMG	Computer Modelling Group.
TVDSS	True vertical depth subsea.
MDT	Modular formation dynamic.
SGS	Sequential Gaussian simulation.
CGR	Condensate gas ratio.
THP	Tubing head pressure.
OGIIP	Original gas initial in place.
HCPV	Hydrocarbons port volume.
SCAL	Lack of special corps.
MER	Maximum efficient rate.
GWC	Gas Water Contact.

Introduction

Introduction

Petroleum Engineering is one of the key aspects of Engineering that is concern with the exploration and production of hydrocarbons from subsurface formations via the wellbore (a hole drilled) to the surface storage facilities for consumption by human or to meet the host country's or global energy needs, it is a broad discipline that has several areas of specializations such as Petroleum geology, Petrophysics, Drilling, Mud and Cementing, Reservoir, Production (surface & subsurface), Completion, Formation evaluation, Economics etc. Thus, all of these areas of specialty work together as an integrated team to achieve one goal; to recover the hydrocarbon in a safe and cost-effective way.

Reservoir engineering is the art of describing quantitatively the behavior of fluids in a porous or fractured rock formation and using that description to effectively manage the production and injection of those fluids. This task is complicated by the fact that no one can be sure of the underground patterns of fractures or porosity that give rise to the permeable channels through which the fluids may move. Furthermore, even if that were possible for one moment, the fracture patterns very likely will change over time since the geothermal environment is a geologically dynamic one.

Reservoir Simulation is a field developed in petroleum engineering where it utilizes porous media in computer modeling to estimate the fluids dynamics, its goal is to predict the field performance under varies producing strategies. Reservoir Simulation is grounded on recognized engineering equations, engineers started calculating reservoir engineering with basic mathematical model long before the emergence of modern technology. Although Reservoir simulation is not new to the industry, it has become more efficient than before due to the advanced capabilities provided by modern day technology. Proficiency, efficiency and effectiveness are the reasons why many engineers became a competent to the model and its development.

The objective is to perform a simulation study in order to determine how best to produce the reservoir over the next 50 years of its life to maximize the gas recovery with as small possible capital investment and operating costs, and the number of wells required to develop the field should be optimized.

To achieve the objectives of this study, a comprehensive integrated multi-disciplinary study was conducted. The study scope included geophysical review, petrophysical evaluations of well logs, a field geo-cellular model construction, reservoir engineering analysis, field reservoir model construction and calibration, and forecast of a conceptual field development plan.

General introduction

We divided our project into three chapters as follows:

In the reservoir and fluid properties chapter which covers the definition of a reservoir and all the basic concepts of reservoir characteristics like the porosity and permeability. Also, it contains the reservoir fluids properties in which we mentioned water and natural gas properties.

The second chapter is titled gas well inflow performance and reserves estimation in place, this topic examines the pressure drop across the reservoir rock between static (shut-in) reservoir pressure and flowing bottomhole pressure. This also includes near wellbore pressure losses due to damage and mechanical "skin" across the perforation tunnels. Pressure loss in the reservoir is referred to as "inflow" and when graphically represented with flowrate is termed the inflow performance relationship. It is used in conjunction with pressure drop in the wellbore ("outflow") for well performance prediction (flowrates and pressures):

At last, the Numerical simulation of reservoirs chapter which is the art of science of using numerical techniques to approach the problems of exploitation of hydrocarbon fields. The main purpose of these numerical techniques is to approximate the solutions of the mathematical equations describing the flow of multiphase fluids in porous media.

Numerical simulation is today one of the most widely used tools in reservoir engineering for:

- Estimate the range of reserves corresponding to different hypotheses on the statics of the reservoir.
- Optimize the development and exploitation scheme of the field according to economic constraints.

Reliable reservoir models are of great importance in making decisions about the management method, they help reduce investment risks during field development and predict performance under various operating conditions.

The objective of this chapter is to build, test, and validate the dynamic simulation model of the GEULLTA-North reservoir of the Ohanet field using Eclipse 100 simulator.

Chapter I:

Reservoir and Fluids Properties

I.1. Definition of a reservoir

A petroleum reservoir is a porous and permeable subsurface pool or formation of hydrocarbon that is contained in fractured rocks which are trapped by overlying impermeable or low permeability rock formation (cap rock, that prevents the vertical movement) and an effective seal (water barrier to prevent the lateral movement of the hydrocarbon) by a single natural pressure system. Figure shows clearly the essential features of a reservoir which are: source rock, cap rock (non-permeable rock), reservoir (porous and permeable rock) rock, hydrocarbon (oil and gas) and aquifer (water sand).[01]

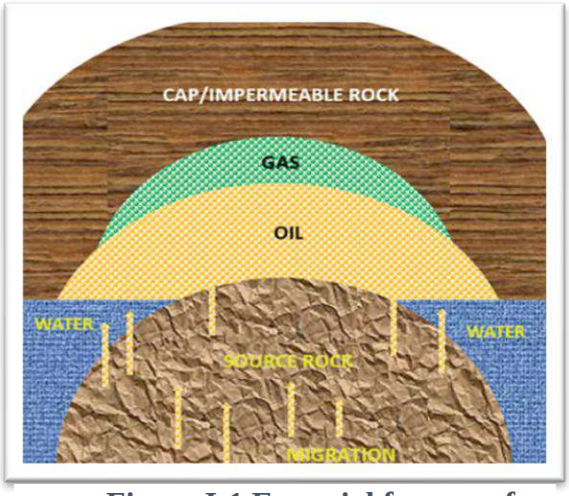

Figure I-1 Essential feature of a reservoir.

I.2. Reservoir characteristics

To form a commercial reservoir of hydrocarbons, a geological formation must possess three essential characteristics;

- Sufficient void space to contain hydrocarbons (porosity).
- Adequate connectivity of these pore spaces to allow transportation over large distances (permeability).
- A capacity to trap sufficient quantities of hydrocarbon to prevent upward migration from the source beds.

I.2.1. Porosity

This is the storage capacity of the rock to host the migrated hydrocarbon from the source rock. It can be defined as the fraction of the bulk volume of the rock that is void or open for fluid to be stored.

The void spaces in the reservoir rocks are, for the most part, the intergranular spaces between the sedimentary particles. Porosity is defined as a percentage or fraction of void to the bulk volume of the rock. While the proportion of void can be calculated from regular arrangements or uniform spheres

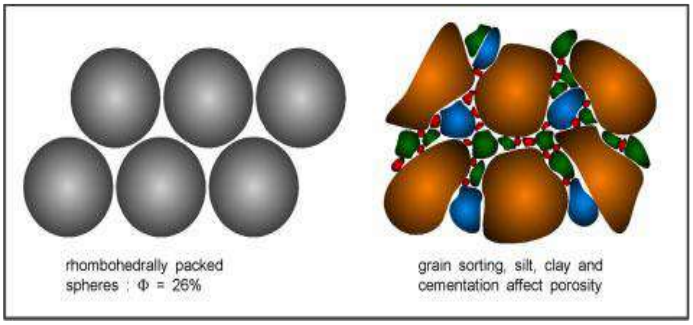

Figure I-2 Intergranular porosity

(see **FigureI.2**), the arrangements within actual reservoirs is a much more complex picture and effected by many different parameters. In this case, measurements are either done in the laboratory on core samples whereby actual conditions are simulated as closely as possible prior to measurement, or in-situ via suites of electric logs such as Neutron, Density and Sonic Logs.

Primary Porosity refers to the void spaces remaining after sedimentation of the granules in the matrix and hence is a matrix porosity.

Secondary Porosity is the contribution from pits, bugs, fractures and other discontinuities in the bulk volume of the matrix. The contribution of secondary porosity to the overall bulk porosity is generally small yet it can lead to dramatic increase in the ease with which hydrocarbons flow through the rock.

From the reservoir engineering point of view, the distinguishing factor between primary and secondary porosity is not the mode of occurrence but the very different flow capacity where an interconnected secondary porosity system is present. This is known as a dual porosity system. In the real world of the reservoir this is often the case and one can easily see how quickly our simulated models can be made complex. Fortunately, in the world of mathematical modeling certain practical assumptions are made to help unbundle this complex approach and best fit the real world to a workable model.[02]

I.2.2. Permeability

Permeability is a measure (under turbulent flow conditions) of the ease with which fluid flows through a porous rock, and is a function of the degree of interconnection between the pores. To illustrate this, **Figure.I .3** shows a volume of rock with the same effective porosity. It is clear that fluid will flow more rapidly through sample A than through sample B where the flow is restricted.

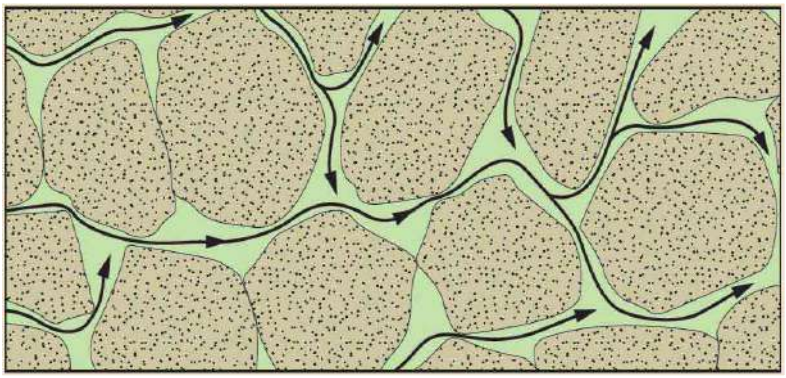

Figure I-3 A volume of rock with the same effective porosity, but drastically different permeabilities

Permeability is measured in Darcy units or more commonly millidarcy (md - one thousandth of a Darcy) after Henry Darcy who carried out some pioneering work on water flow through unconsolidated sand stones.

Like porosity, permeability can be measured in the laboratory from core samples. There is to date no instrument which measures permeability directly in-situ, but permeability can be calculated via complex differential equations after subjecting the reservoir to a dynamic condition

and monitoring the corresponding pressure and temperature response. While grain size has a negligible effect on the porosity of a rock, this parameter has a predominant effect on permeability. This is so because as we are dealing with flow, we are also dealing with friction of the fluid against the surface area of the rock grains. Each rock grain has a wetted surface surrounding it where fluid velocity is always zero by definition, thus shearing friction is formed between this zero-velocity layer and any passing fluids. Thus, more frictional forces are encountered passing the same fluid through a fine granular pack than through a coarse granular pack of equal porosity. See **FigureI.4**.

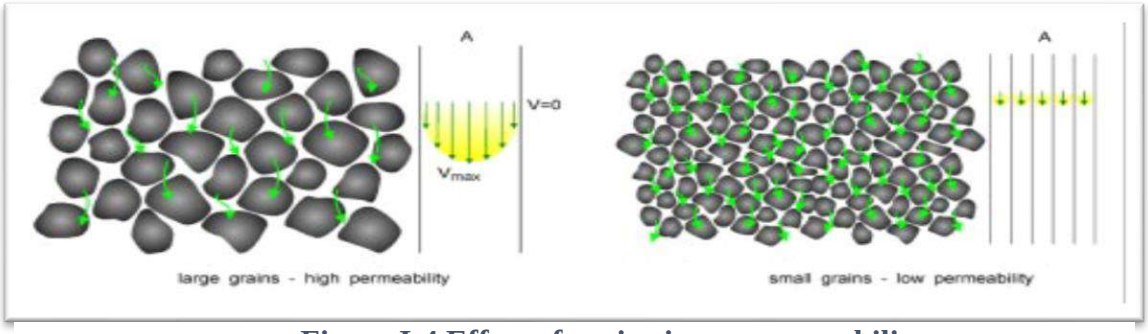

Figure I-4 Effect of grain size on permeability

Similarly, one can understand that the apparent permeability will also be dependent on the type of fluid flowing through the rock and this plays an important part in the interpretation of different hydrocarbon bearing reservoirs. Permeability is denoted in three different ways. Absolute permeability ka is derived in the laboratory by flowing a known quantity of fluid through a core while its pore spaces are 100% saturated with the same fluid. Absolute permeability will not change with varying fluids as long as the pore space configuration remains constant.

Effective permeability is the permeability of a flowing phase which does not saturate 100% of the rock. The effective permeability is always less than the absolute value of k for the rock.

Relative permeability is a dimensionless number which is the ratio of effective permeability (to a fluid) to absolute permeability of the same rock.

I.3. Reservoir fluids properties

Reservoir fluid properties are normally measured in the laboratory. Pressure-Volume-Temperature (PVT) properties relate these properties to each other at equilibrium conditions. These variables, typically used for volumetric related reservoir behavior, are measured in a laboratory PVT Cell. A PVT Cell is a high-pressure vessel (container) that allows for the control and measurement of pressure, volume, and temperature.[03]

In addition to laboratory measurements, reservoir PVT properties can be determined from Equations-of-State (EOS). Equations-of-state are theoretically derived equations that relate the State Variables: pressure, volume, and temperature (state variables are variables that define the thermodynamic state of a system). Three common examples of equations-of-state include:

Isothermal compressibility:

$$c_f = \frac{-1}{V_f}\frac{dV_f}{dp}\Big]_{T=\text{ constant}} \quad ; V_{fref}e^{-c_f(p-p_{ref})} \approx V_{fref}[1 - c_f(p - p_{ref})] \qquad \text{Eq.I.01}$$

Real Gas Law:

$$pV = ZnRT \qquad \text{Eq.I.02}$$

Van der Waal's Cubic EOS:

$$\left[p + a\left(\frac{n}{V}\right)^2\right]\left(\frac{V}{n} - b\right) = RT \qquad \text{Eq.I.03}$$

In **Equation 01**, the negative sign is required because the volume of a fluid decreases as pressure increase (i.e., the derivative is negative). Note that all of these relationships allow for the determination of one of the state variables, p, V, or T, if the two other variables are known (two degrees of freedom). For the isothermal compressibility EOS, **Equation 01**, temperature can be considered a variable if we have tables or equations where the value of c_f can be defined for a specific temperature.

In addition to the equations-of-state, fluid PVT correlations are also used in the oil and gas industry. These correlations can be either graphical or mathematical in nature. Fluid property correlations are simply plots, curve fits, or regressions of many laboratory measurements covering a wide range of data. In general, these correlations may not be as accurate as laboratory measurements or equations-of-state, but they have their uses in reservoir engineering.

I.3.1. Water properties

All oil and gas reservoirs have water associated with them. Since it is a common part of the system, we will need to discuss how it is stored and moves in the reservoir.

I.3.1.1. Water formation volume factor, Bw

The water (or more correctly, the brine) Formation Volume Factor, B_w, (sometimes referred to as the FVF) is a pressure and temperature dependent property that relates the volume of 1.0 stock tank barrel, STB, of water to its volume in barrels, bbl, at another pressure. It has the units of bbls/STB. We have already discussed the use of the stock tank pressure and temperature as an oilfield reference system.

By definition, if we had 1.0 STB of water at p_{ST} and T_{ST}, and that same STB occupied 1.02 bbls at reservoir conditions, p_r and T_r, then it would have a formation volume factor of:

$$B_w(p_r, T_r) = \frac{V_{wr}bbl}{V_{wST}STB} = \frac{1.02bbl}{1.00STB} = 1.02bbl/STBWe$$

$$B_w(p_r, T_r) = \frac{V_{wr}\text{bbl}}{V_{wST}\text{STB}} = \left(\frac{m_{1STB}\text{lb}}{\rho_{wr}\text{lb/bbl}}\right)\left(\frac{\rho_{wSTB}\text{lb/STB}}{m_{1STB}\text{lb}}\right) = \frac{\rho_{wST}\text{lb/STB}}{\rho_{wr}\text{lb/bbl}};\ \text{in bbl/STB} \quad \text{Eq.I.04}$$

which implies:

$$\rho_w(p_r, T_r) = \frac{\rho_{wST}}{B_w}(\text{lb/bbl});\ \text{or}\ \rho_w(\rho_r, T_r) = \frac{\rho_{wST}}{5.615 B_w}(\text{lb/ft}^3) \quad \text{Eq.I.05}$$

I.3.1.2. Water isothermal compressibility, cw

Water is considered to be a slightly compressible liquid with a very low value of compressibility. From **Equation I.01** we have:

$$c_w = -\frac{1}{V_w}\frac{dV_w}{dp}\Big]_{T=\text{ constant}} \quad \text{Eq.I.06}$$

One correlation for water compressibility, c_w, is:

$$c_w = (7.033p + 541.5C - 537.0T + 403.3 \times 10^3)^{-1} \quad \text{Eq.I.07}$$

Where:

- p is the pressure, psi
- C is the salt concentration, gm/L
- T is temperature, °F

We can develop an explicit formula for the water formation volume factor based on the water compressibility.[04] If we take 1.0 STB of water and its volume in barrels at a reservoir pressure and temperature, then we would have: V_w (bbl) = B_w (p_r, T_r) (bbl/STB) x 1.0 STB. Now,

$$c_w = -\frac{1}{V_w}\frac{dV_w}{dp}\Big]_{T=\text{ constant}} = -\frac{1}{(B_w)(1STB)}\frac{d[(B_w)(1STB)]}{dp}\Big]_{T=T_{res}} = -\frac{1}{B_w}\frac{dB_w}{dp}\Big]_{T=T_{res}} \quad \text{Eq.I.08}$$

Or,

$$B_w(p, T_r) = B_{wref}[1 - c_w]_{pref,Tr}(p - p_{ref})] \quad \text{Eq.I.09}$$

I.3.1.3. Water Viscosity, μw

In the laboratory, the water viscosity is measured with an apparatus called a Viscometer. The mechanics and test procedures for a viscometer are beyond the scope of this course, and we will work with known correlations. One correlation from McCain has the form:

$$\mu_{w14.7psi} = AT^{-B} \quad \text{Eq.I.10}$$

With

$$A = 109.574 - 8.40564S + 0.313314S^2 + 8.72213 \times 10^{-3}S^3 \quad \text{Eq.I.11}$$

And

$$B = 1.12166 - 2.63951 \times 10^{-2}S + 0.313314S^2 + 6.79461 \times 10^{-4}S^2 + 5.47119 \times 10^{-5}S^3 - 1.55586 \times 10^{-6}S^4 \quad \text{Eq.I.12}$$

Where:

- $\mu_{w\ 14.7\ psi}$ is the water viscosity at 14.7 psi and temperature, T °F
- S is the salt concentration in weight percent, W_t% (note different unit from **Equation.I. 7**)

Once the viscosity at 14.7 psi and T °F are determined, the water viscosity at other pressures can be determined from:

$$\frac{\mu_w}{\mu_{w14.7psi}} = 0.9994 + 4.0295 \times 10^{-5}p + 3.1062 \times 10^{-9}p^2 \quad \text{Eq.I.13}$$

I.3.1.4. Water density, ρw

The density of water is also a property of interest in petroleum engineering. McCain provides the following correlation for estimating the water density at reference conditions:

$$\rho_{wST} = 62.368 + 0.438603S + 1.60074 \times 10^{-9}S^2 \quad \text{Eq.I.14}$$

Where:

- $\rho_{w\ ST}$ is the water density at sock tank conditions, lb/ft^3
- S is the salt concentration in weight percent, Wt%

The water density at reservoir conditions can then be calculated using **Equation.I. 5**.

I.3.2. Natural gas properties

For natural gases we are also most interested in the Gas Formation Volume Factor, B_g, and the Gas Viscosity, μ_g, as these properties strongly influence gas storage (and accumulation) and gas flow. For most reservoir engineering calculations, the gas formation volume factor (and Gas Compressibility, c_g, and Gas Density, ρ_g) can be determined from the Real Gas Law, **Equation I. 2**:

$$pV = ZnRT$$

Where:

- p is the pressure of interest, psi
- V is the volume, ft^3
- Z is the oil super-compressibility factor, dimensionless
- R is the gas constant, (psi ft^3) / (lb-moles °R)
- T is temperature, °R (°R = °F + 460.67)

I.3.2.1. Gas super-compressibility factor, Z

The gas super-compressibility factor, Z (or Z-Factor, or Real Gas Deviation Factor), is a function of pressure and temperature that corrects the Ideal Gas Law for high pressure and high temperature conditions. In the oil and gas industry, the z-factor correlation for hydrocarbon gases

that is universally accepted in the Standing-Katz Correlation. This correlation is shown graphically in **FigureI.5**.

As illustrated in **Figure I.5** The Standing-Katz Correlation correlates the z-factor to the Pseudo-Reduced Pressure, p_{pr}, and Pseudo-Reduced Temperature, T_{pr}. The pseudo-reduced properties are defined by:

$$P_{pr} = \frac{P}{P_{pc}} \quad \text{Eq.I.15}$$

And

$$Tpr = T/Tpc \quad \text{Eq.I.16}$$

Where:

- p is the pressure of interest, psi
- p_{pc} is the pseudo-critical pressure, psi
- T is temperature of interest, °R
- T_{pc} is pseudo-critical temperature, °R

All of these properties are called pseudo-properties because the pseudo-critical pressure and pseudo-critical temperature are not the true, measured critical properties, but are calculated properties:

$$P_{pc} = 756.8 - 131.0\gamma_g - 3.6\gamma_g^2 \quad \text{Eq.I.17}$$

And

$$T_{pc} = 169.2 + 349.5\gamma_g - 74.0\gamma_g^2 \quad \text{Eq.I.18}$$

With

$$\gamma_g = \frac{MW_g}{MW_{air}} = \frac{MW_g}{28.97} \quad \text{Eq.I.19}$$

Where:

- p_{pc} is the pseudo-critical pressure, psi
- T_{pc} is the pseudo-critical temperature, °R
- Υ_g is the gas gravity (MW_g/MW_{air}), dimensionless
- MW_g is the molecular weight of the gas, lb/lb-mole
- MW_{air} is the molecular weight of air, lb/lb-mole (28.97 lb/lb-mole)

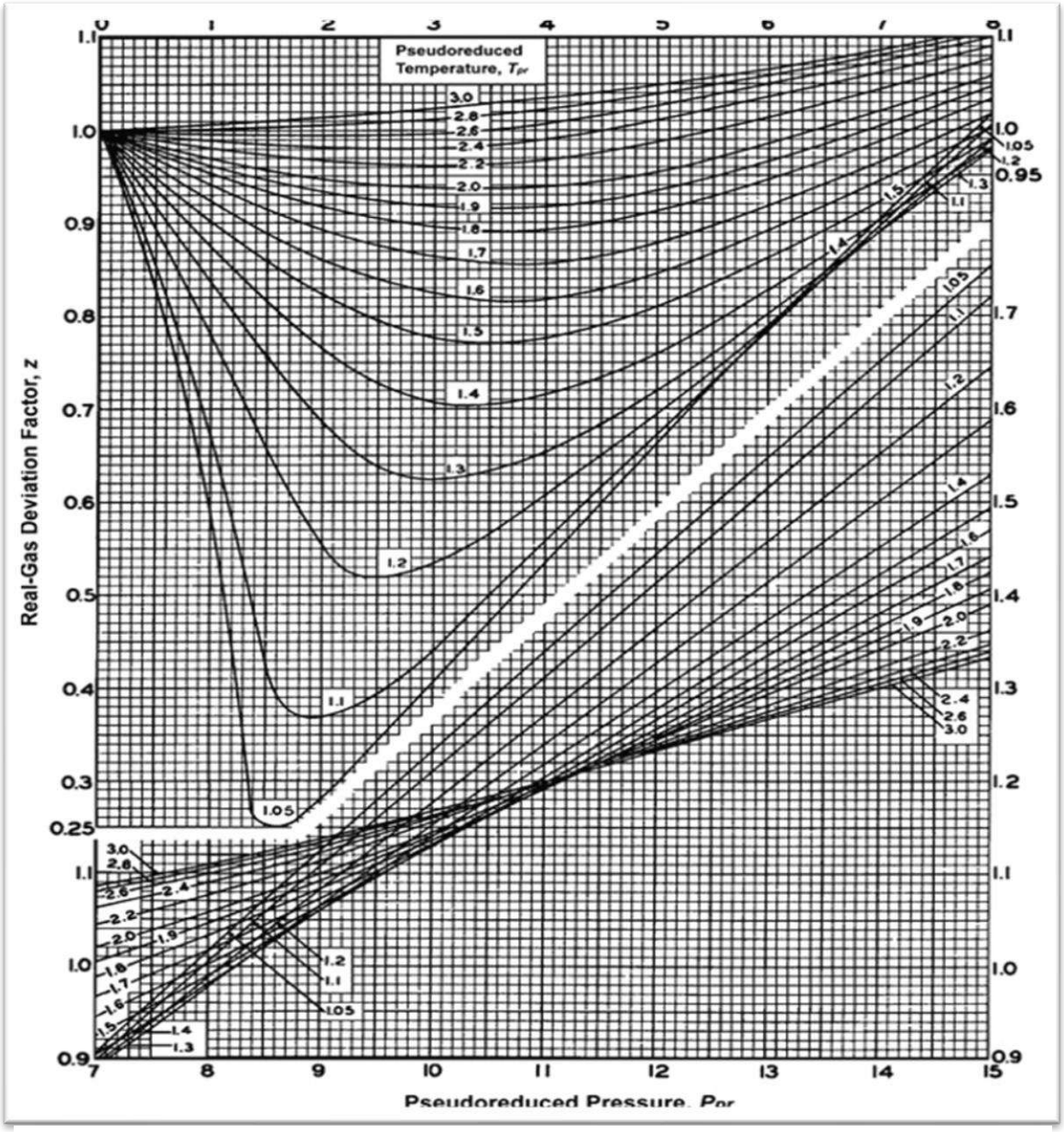

Figure I-5 Standing-Katz Correlation for Z-Factors of Hydrocarbon Gases, Source: Greg King

In cases where significant concentrations of inorganic impurities, CO_2 and H_2S are present, then corrections to **Equation I.17** and **Equation I.18** are required:

$$P_{\text{pc corrected}} = \frac{P_{pc\ \text{Eq.3.60}}\, T_{pc\ \text{corrected}}}{T_{pc\ \text{Eq.3.61}} + y_{H_2S}\left(1 - Y_{H_2S}\right)\varepsilon_{\text{correction}}} \qquad \text{Eq.I.20}$$

And

$$T_{pc\ \text{corrected}} = T_{pc\ \text{Eq.3.61}} - \varepsilon_{\text{correction}} \qquad \text{Eq.I.21}$$

With

$$\varepsilon_{\text{correction}} = 120.0\left[\left(y_{co_2} + y_{H_2S}\right)^{0.9} + \left(y_{co_2} + y_{H_2S}\right)^{1.6}\right] + \left(y_{H_2S}^{0.5} + y_{H_2S}^{4.0}\right) \qquad \text{Eq.I.22}$$

Where:

- $P_{pc\ corrected}$ is the corrected pseudo-critical pressure, psi
- $P_{pc\ Eq.\ 41}$ is the pseudo-critical pressure from **Equation I.19**, psi
- $T_{pc\ corrected}$ is the corrected pseudo-critical temperature, °R
- $T_{pc\ Eq.\ 40}$ is the corrected pseudo-critical from **Equation I.18**, °R
- $\epsilon_{correction}$ is the correction for CO_2 and H_2S, °R
- y_{CO2} is the mole fraction of CO_2 in the gas phase, fraction
- y_{H2S} is the mole fraction of H_2S in the gas phase, fraction

The Standing-Katz correlation has also been mathematically curved fit. The equation for z-factor then becomes:

$$\begin{aligned} Z = 1.0 + (&0.3265 - 1.0700T_{pr}^{-1} - 0.5339T_{pr}^{-3} + 0.01569T_{pr}^{-4} - 0.05165T_{pr}^{-5})\rho_{pr} \\ &+\left(0.5475 - 0.7361T_{pr}^{-1} + 0.1844T_{pr}^{-2}\right)\rho_{pr}^{2} \\ &-0.1056\left(-0.7361T_{pr}^{-1} + 0.1844T_{pr}^{-2}\right)\rho_{pr}^{5} \\ &+0.6134\left(1.0 + 0.7210\rho_{pr}^{2}\right)\left(\rho_{pr}^{2}T_{pr}^{-3}\right)e^{-0.7210\rho_{pr}^{2}} \end{aligned} \quad \text{Eq.I.23}$$

With

$$\rho_{pr} = 0.27\frac{P_{pr}}{ZT_{pr}} \quad \text{Eq.I.24}$$

It should be noted that the solution of this equation for the z-factor requires an iteration procedure. This is because the z-factor appears both on the left-hand side of **Equation I.24** and the right-hand side of the equation through the pseudo-reduced density, ρ_{pr}. Typically, this is solved with a Newton-Raphson iteration procedure which is beyond the scope of this class.[05] For our purposes, if super-compressibility factors are required, we can simply read the chart to obtain them.

I.3.2.2. Real gas formation volume factor, B_g

The Formation Volume Factor, B_g, of a real gas, like its oil phase analog, is used to convert one standard cubic foot, SCF, of gas at reference conditions to its volume at reservoir conditions. For natural gases, in the U.S. domestic oil and gas industry, we use the standard conditions of P_{SC} = 14.7 psi and 60 °F. The gas formation volume factor for a real gas can be calculated directly from the Real Gas Law once we have an estimate of the super-compressibility factor. If we assume one lb-mole of natural gas, then the volume that it would occupy at standard conditions would be (assuming Z_{SC} = 1.0 at standard conditions – a very good assumption):

$$V_{SC} = \frac{Z_{SC}nRT_{SC}}{p_{SC}} = \frac{nRT_{SC}}{p_{SC}} \text{ in ft}^3;\ \text{with } Z_{SC} = 1.0 \quad \text{Eq.I.25}$$

At reservoir conditions, that same lb-mole would occupy a volume of:

$$V_r = \frac{ZnRT_r}{p_r} \text{in} ft^3 \quad \text{Eq.I.26}$$

Now, the gas phase formation volume factor we can define as:

$$B_g = \frac{V_r}{V_{SC}} = \frac{ZnRT_r p_{SC}}{nRT_{SC} p_r} = Z\frac{T_r p_{SC}}{T_{SC} p_r} \text{ in } ft^3/SCF \quad \text{Eq.I.27}$$

There are times when we would like to consider the volume of gas in reservoir barrels, bbl. This is because we have used reservoir barrels as the units for the liquid (oil and water) volumes, and we would like to determine the volume occupied by the gas and liquids combined. We can convert the units of **Equation 27** by applying the unit conversion constant of 1 bbl = 5.615 ft^3:

$$B_g = \frac{Z}{5.615}\frac{T_r p_{SC}}{T_{SC} p_r} \text{ in bbl/SCF} \quad \text{Eq.I.28}$$

Where:

- B_g is the gas formation volume factor, ft^3/SCF (**Equation I.27**) or bbl/SCF (**Equation I.28**)
- Z is the super compressibility factor at reservoir conditions, p_r and T_r, dimensionless
- T_r is the reservoir temperature, °R
- T_{SC} is the reference (standard) temperature (520 °R in U.S. domestic industry), °R
- p_r is the reservoir pressure, psi
- p_{SC} is the reference (standard) pressure (14.7 psi in the U.S. domestic industry), psi

I.3.2.3. Real gas compressibility, c_g

The isothermal compressibility of a real gas can also be determined directly from the Real Gas Law. Starting with the definition of isothermal compressibility:

$$c_g = -\frac{1}{V_g}\frac{dV_g}{dp}\Big]_{T=\text{ constant}} \quad \text{Eq.I.29}$$

Substituting the Real Gas Law, **Equation I.2**, into **Equation I.30**:

$$c_g = -\frac{p}{ZnRT_r}\frac{d}{dp}\left(\frac{ZnRT_r}{p}\right)\Big]_{T=T_r} \quad \text{Eq.I.30}$$

Or

$$c_g = -\frac{p}{Z}\frac{d}{dp}\left(\frac{Z}{p}\right)\Big]_{T=T_r} = \frac{1}{p} - \frac{1}{Z}\frac{dZ}{dp} \quad \text{Eq.I.31}$$

The derivative, dZ/dp, can be calculated by differentiating **Equation I.23** and **Equation I.24** with respect to pressure.

I.3.2.4. Real gas density, ρ_g

The density of a real gas can also be determined directly from the Real Gas Law. Starting with the Real Gas Law:

$$pV = ZnRT$$

Now the number of moles is equal to a mass divided by the molecular weight, n = m / MWg. Substituting into the Real Gas Law:

$$pV = \frac{ZmRT}{MW_g}$$

Now from the definition of gas density and the substitution of the Real Gas Law:

$$\rho_g = \frac{m}{V} = \frac{pMW_g}{ZRT} \qquad \text{Eq.I.32}$$

Where:

- ρ_g is the gas density, lb/ft^3
- p is the pressure of interest, psi
- MW_g is the molecular weight of the gas, lb/lb-mole
- Z is the super compressibility factor at reservoir conditions, p_r and T_r, dimensionless
- R is the Gas Constant, 10.73 ft^3 psi / °R lb-mole
- T is the temperature of interest, °R

I.3.2.5. Real gas specific gravity, γ_g

The specific gravity of a real gas can also be determined directly from the Real Gas Law. For gases, the specific gravity is defined as the ratio of the density of the gas to the density of air at standard conditions. Dividing **Equation I.32** written for a gas. written for air at standard conditions (Z = 1.0) results in:

$$\gamma_g = \frac{\rho_g}{\rho_{air}} = \frac{\left(\frac{p_{SC}MW_g}{RT_{SC}}\right)}{\left(\frac{p_{SC}MW_{air}}{RT_{SC}}\right)} = \frac{MW_g}{MW_{air}} \qquad \text{Eq.I.33}$$

Now, the molecular weight of gas is 28.87 lb/lb-mole:

$$\gamma_g = \frac{MW_g}{28.97} \qquad \text{Eq.I.34}$$

I.3.2.6. Real gas viscosity, µg.

The viscosity of natural gases can be determined by the correlation of Lee, Gonzalez, and Eakin:

$$\mu_g = 1.0 \times 10^{-4} K e^{X\rho_g^Y} \qquad \text{Eq.I.35}$$

With

$$K = \frac{(9.379 + 0.01607MW_g)T^{1.5}}{209.2 + 19.26MW_g + T} \quad \text{Eq.I.36}$$

$$X = 3.448 + \frac{986.4}{T} + 0.01009MW_g \quad \text{Eq.I.37}$$

$$Y = 2.447 - 0.2224X$$

Where:

- μ_g is the gas viscosity, cp
- K, X, and Y are correlation coefficients
- ρ_g is the gas density at the pressure and temperature of interest, gm/cc [ρg(gm/cc) =1.4935×10−3MWg pzT] [ρg(gm/cc) =1.4935×10−3MWg pzT]
- MW_g is the molecular weight of the gas, lb/lb-mole
- T is the temperature of interest, °R

Chapter II:

Gas Well Inflow Performance and Reserves Estimation in Place

II.1. Reservoir fluid flow fundamentals

Pressure loss in the reservoir is commonly called “drawdown” and can be divided into flowrate to provide a ratio called the productivity index (PI).

Productivity index (PI) is defined as flowrate divided by reservoir pressure drop (drawdown): $PI = \frac{Q}{(P_g - P_\mu)} [\text{stb}// \text{ day }]/[\text{psi}]$ Eq.II.01

For oil wells, PI is usually linear above the bubble point and can be easily matched to measured data. Below the bubble point, PI decreases due to effect of gas bubbles causing an extra pressure drop.

Note that the flowrate is always expressed in standard conditions of liquid (i.e., stbl/d or sm^3l/d):

Below the bubble point, the Vogel IPR (based on empirical data) is often used to account for the decrease in PI due to gas.

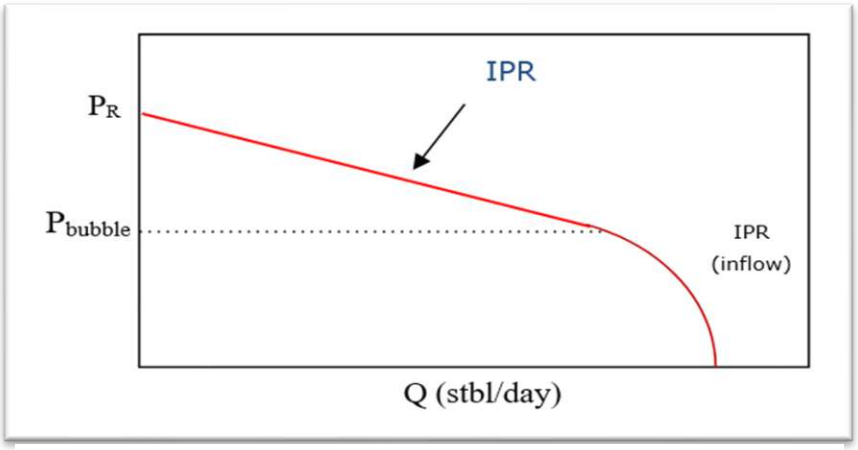

Figure II-1 : IPR below the bubble point curve

For an existing well, PI can be obtained from a measurement of bottomhole pressure (P_{wf}), reservoir pressure (P_R) and flowrate (Q).

If P_{wf} is not measured, it can be calculated from WHP using the flow correlations for pressure drop in the wellbore.[06]

II.2. Darcy’s law

For a new well, PI can be estimated by using Darcy's law.

Darcy was an engineer working for the city of Dijon on water supply systems (1850’s). He was interested in finding which types of sand provided the most effective filtration with minimum pressure loss. He made measurements of pressure drop along a length of horizontal pipe filled with various sand types and derived the following relationship:

$$Q = k \cdot \frac{A}{L} \cdot h$$ Eq.II.02

With:

k: permeability

A: the filter section

L: the length of the filter

h: the difference at the piezometric head

Darcy's law is generalized for the oil field, this law stipulates that the volume flow is proportional to the pressure difference according to the following relationship:

$$Q = k \cdot \frac{A}{\mu} \cdot \frac{\Delta P}{\Delta x} \qquad \text{Eq.II.03}$$

This is effectively a friction pressure drop relationship (see pressure drop in wellbore) with the addition of permeability to account for the flow resistance of the sand.

A few years after Darcy published this relationship, the first oil well was drilled in the US and it was recognized that this could be used for radial flow in reservoirs with a few modifications for the flow geometry.

Darcy's law for radial, single phase reservoir flow in oilfield units is:

$$P_r - P_{\psi j} = \frac{141.2 \cdot Q \cdot B_a \cdot \mu \left\{ \ln\left(\frac{r}{r_\psi}\right) + s \right\}}{k \cdot h} \qquad \text{Eq.II.04}$$

where:

Q = flowrate (stb/day)

B_o = FVF (rb/stb)

M = viscosity (cP)

k = permeability (mD)

h = thickness (feet)

r = res. radius (feet) r_w = well radius (feet) s = skin

Oil volume factor is added to account for the in-situ volume (reservoir barrels, rb/d) rather than stb/d. In radial flow, the flow length is between the reservoir drainage boundary (r) and the wellbore radius (r_w).

The term "s" or skin is added to account for any pressure drops not accounted for in the simple assumptions of Darcy's law.

II.3. Skin

Skin is the extra pressure drop between P_{wf} in the center of the wellbore and the pressure at the undamaged rock formation i.e., within a meter of the wellbore.

Skin is a dimensionless number which indicated the degree or amount of extra pressure drop.

Skin has three components: mechanical damage (+), partial penetration (+) and deviation (-).

This "near wellbore" or mechanical damage could be caused by the following:

- gravel pack blockage
- scale or sand build-up
- blocked perforation tunnels
- mud filtrate invasion (from drilling mud)

A general expression of the skin factor is

$$S = S_D + S_{C+\theta} + S_P + \sum S_{PS} \qquad \text{Eq.II.05}$$

where S_D is damage skin during drilling, cementing, well completion, fluid injection, and even oil and gas production. Physically, it is due to plugging of pore space by external or internal solid particles and fluids. This component of skin factor can be removed or averted with well stimulation operations. The $S_{C+\theta}$ is a skin component due to partial completion and deviation angle, which make the flow pattern near the wellbore deviate from ideal radial flow pattern. This skin component is not removable in water coning and gas coning systems. The S_P is a skin component due to the nonideal flow condition around the perforations associated with cased-hole completion. It depends on a number of parameters including perforation density, phase angle, perforation depth, diameter, compacted zone, and others. This component can be minimized with optimized perorating technologies. The ΣS_{PS} represents pseudo-skin components due to non–Darcy flow effect, multiphase effect, and flow convergence near the wellbore. These components cannot be eliminated.[07]

II.4. Gas well inflow performance

The inflow performance relationship for gas wells is more complex than for oil wells, primarily due to the compressible nature of the fluid. The IPR curve is non-linear and is illustrated as follows:

An early (1930s) empirical analysis of gas wells by Schellhardt and Rawlins resulted in the "back pressure" or "C and n" equation:

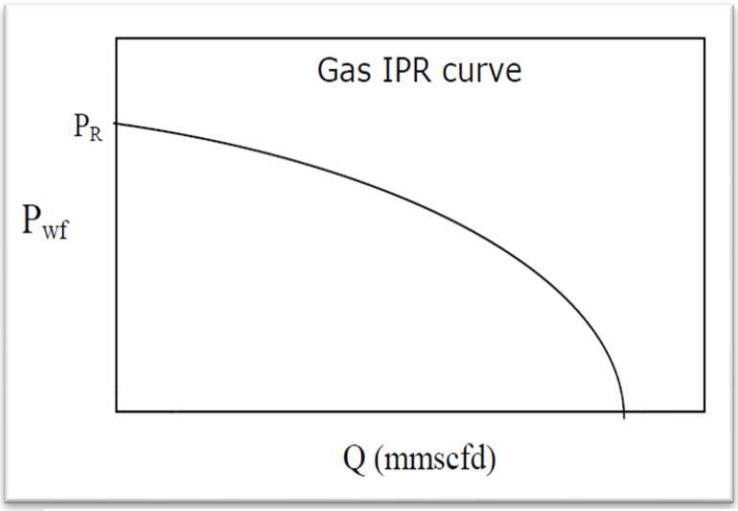

Figure II-2: Gas IPR curve

Where:

$Q = C. (P_R^2 – P_{wf}^2)^n$

Q = gas flowrate

P_R = static reservoir pressure P_{wf} = flowing well face pressure

C = function of k, h, μ, z, s, r/rw

n = non-Darcy flow function (range 0.5 to 1)

Although this equation is an approximation, it illustrates the basic dependencies of the gas IPR curve.

The derivation of Darcy's law for gas wells is complex, since many of the assumptions used to linearize the equation for oil (i.e., that viscosity and compressibility are independent of pressure) are invalid for gases.

In order to assist with solving the equation for gas, the concept of "real gas pseudo pressure" or m(p) was introduced by Al-Hussainy, Ramey and Crawford (1966).

$$m(p) = 2 \int_{p_b}^{p} p \cdot \frac{dp}{\mu} \cdot z \qquad \text{Eq.II.06}$$

Where:

m(p) = real gas pseudo pressure p = pressure

P_b = base pressure

Using this approach, the semi-state reservoir inflow equation for gas wells can be expressed

as:

$$m(p_r) - m(p_{wf}) = \frac{1422 \cdot Q \cdot T}{k \cdot h}\left(\frac{\ln r}{r_w} - \frac{3}{4} + S\right) \quad \text{Eq.II.07}$$

Where:

Q = gas flowrate (mscfd)

T = absolute temperature

S = mechanical skin factor

For high-rate gas wells, an additional complication is the rate dependency of the skin factor (due to velocity causing increasing frictional pressure loss). This can be added to the above equation as a "rate dependent skin factor" or a "non-Darcy flow coefficient":

$$m(p_r) - m(p_{wf}) = \frac{1422 \cdot Q \cdot T}{k \cdot h}\left(\frac{\ln r}{r_w} - \frac{3}{4} + S\right) + F \cdot Q^2 \quad \text{Eq.II.08}$$

or

$$m(p_r) - m(p_{wf}) = \frac{1422 \cdot Q \cdot T}{k \cdot h}\left(\frac{\ln r}{r_w} - \frac{3}{4} + S + D \cdot Q\right) \quad \text{Eq.II.09}$$

Where:

$F.Q^2$ = non-Darcy flow coefficient

D.Q = rate dependent skin factor D and F are determined from multi-rate tests.

II.5. Well testing

Well testing involves taking and analyzing bottomhole pressure and rate measurements for flowing and shut-in conditions.

A multi-rate test for gas wells can be used to match the IPR model, i.e., determining C and n for the back pressure equation or D and F for the turbulent Darcy model:

Tests should ideally be carried out at a wide variety of rates and should be stabilized as much as possible (minimum flow period of 4 hours). Low permeability reservoirs may take some time to stabilize and require at least 24 hours for each flow period. Gauge pressures should be corrected to the well or reservoir datum depth (P_{wf}) using appropriate flow correlations.[08]

For oil wells, multi-rate testing will derive the productivity index (PI).

The most important factors that can be calculated from multi-rate testing include permeability (k) and skin (s). This is especially true on the initial testing of the well potential during a drill stem test (DST).

II.5.1. Pressure build-up and drawdown analysis

A simple but very critical set of data measurements can be made by flowing the well for a period and then shutting the well in and accurately recording the pressure build up with a gauge

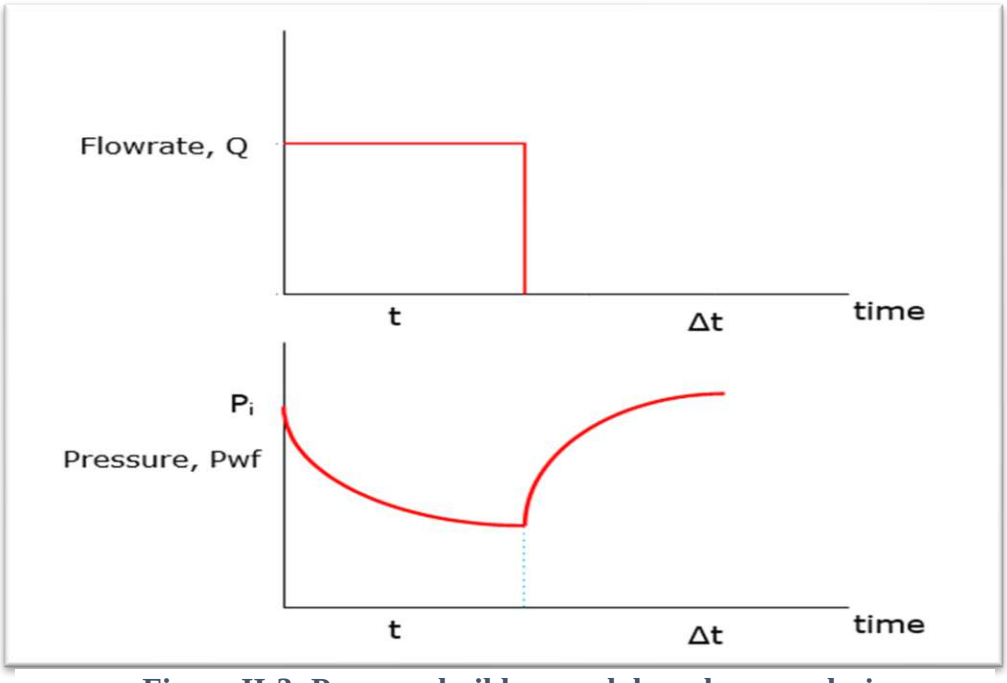

Figure II-3: Pressure build-up and drawdown analysis

as close to the reservoir as possible. Quartz gauges are commonly used to ensure high resolution of pressure measurement.

For the flowing period (drawdown), the following equation applies

$$2.\pi \cdot k \cdot h\left(P_i - P_{wf}\right) = p_D(t_D) + Sq \cdot \mu \qquad \text{Eq.II.10}$$

from which k, h and s can be derived (usually by plotting).

For the shut-in period (build up), the following equation applies:

$$2.\pi \cdot k \cdot h\left(P_i - P_{wf}\right) = p_D(t_D + \Delta t_D) - p_D(\Delta t_D)q \cdot \mu \qquad \text{Eq.II.11}$$

This is the basic pressure build up equation and is usually solved by plotting the build-up pressure (P_{wf}) against log (t + Δt)/ Δt) which is called the Horner Plot (1951):

P^* represents the extrapolation of the pressure data to infinite time. This is a theoretic concept and the true static reservoir pressure is likely to be somewhat lower, as represented by P_{av}.

An alternative method for pressure build-up analysis is given by the Miller-Brons-Hazelbrook (MBH) method (1949, 1954) in which the buildup pressure is plotted against ln Δt.

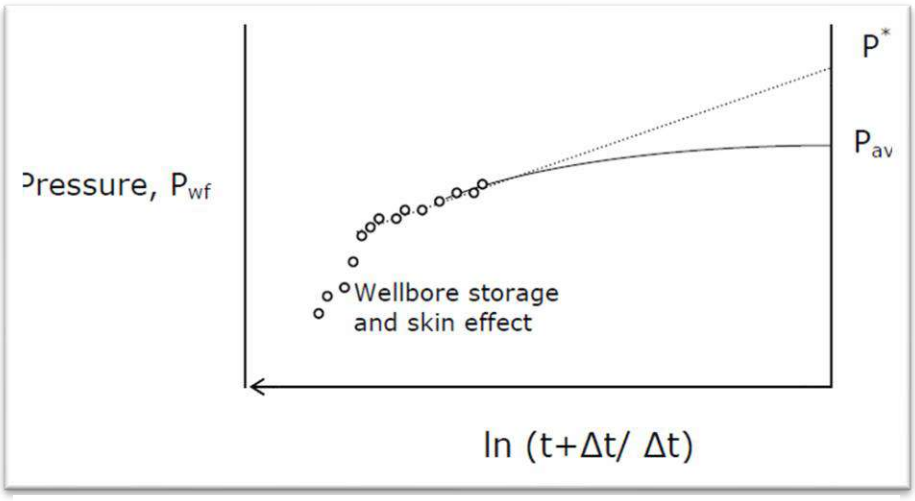

Figure II-4: The build-up test on Honer's plot

II.5.2. Derivative analysis techniques

In the 1980's the technique of pressure derivative analysis was developed to assist in the identification of the linear transient phase of pressure drawdown/build up i.e., examining the rate of change of the pressure response.

.A huge number of theoretical responses were generated representing various reservoir types and configurations that became known as "type curves". Superposition of measured data over these curves could be used to more quickly identify the type of the reservoir response.

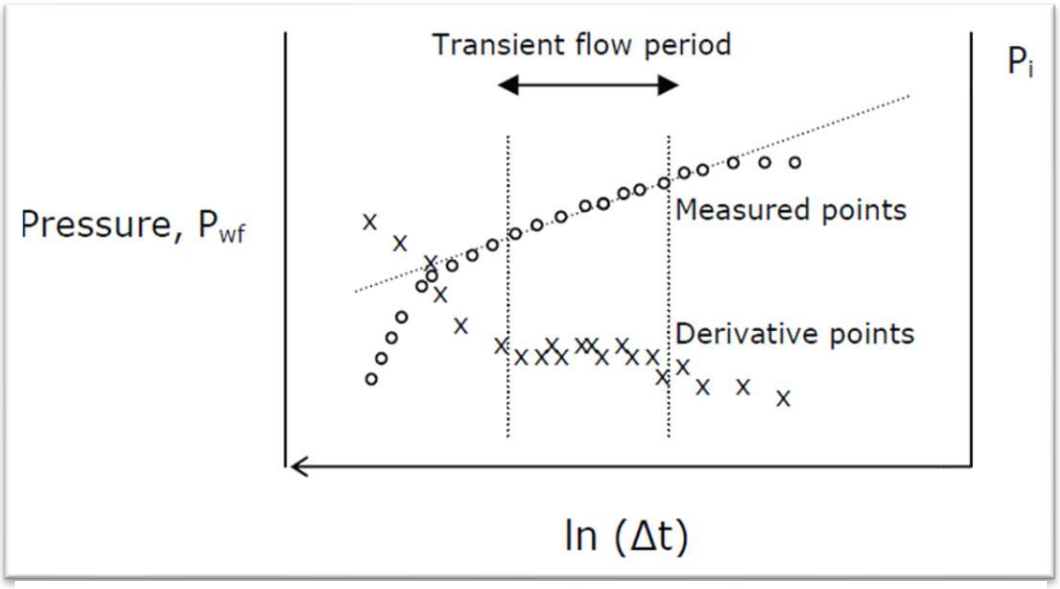

Figure II-5 : Pressure derivate analysis curve

II.6. Reserves estimation in place

To better understand reserves estimation, a few important terms require definition. Original gas in place (OGIP) refer to the total volume of hydrocarbon stored in a reservoir prior to production. Reserves or recoverable reserves are the volume of hydrocarbons that can be profitably extracted from a reservoir using existing technology. Resources are reserves plus all other hydrocarbons that may eventually become producible; this includes known oil and gas deposits present that cannot be technologically or economically recovered (OGIP) as well as other undiscovered potential reserves.[09]

Estimating hydrocarbon reserves is a complex process that involves integrating geological and engineering data. Depending on the amount and quality of data available, one or more of the following methods may be used to estimate reserves:

- Volumetric
- Material balance
- Analogy

These methods are summarized in **Table II.1**

Table II-1: Summary of methods used to derive hydrocarbon reserves

Method	Application	Accuracy
Volumetric	OGIP, recoverable reserves. Use early in life of field.	Dependent on quality of reservoir description. Reserves estimates often high because this method does not consider problems of reservoir heterogeneity.
Material balance	OGIP (assumes adequate production history available), recoverable reserves (OGIP known). Use in a mature field with abundant geological, petrophysical, and engineering data.	Highly dependent on quality of reservoir description and amount of production data available. Reserve estimates variable.
Analogy	OGIP, recoverable reserves. Use early in exploration and initial field development.	Highly dependent on similarity of reservoir characteristics. Reserve estimates are often very general.

II.6.1. Volumetric technique

The volumetric technique is one of the most straightforward methods to estimate gas initially in place (GIIP) because the main principle is simple, requires limited data and does not need dynamic reservoir data such as flowing bottom hole pressures or production flow rates. The essential data for applying the volumetric method are structural and stratigraphic cross-sectional maps, well logs, core tests, fluid sample analysis, and well tests. The contour maps and well logs are employed to calculate the bulk volume, the porosity measurements lead to converting the bulk volume to pore volume, the resistivity logs define the water saturation in the pores to estimate the gas volume at reservoir conditions, and the fluid sample analysis and pressure-volume-temperature correlations calculate the gas formation volume factor that converts GIIP from initial reservoir conditions to standard conditions.

The volumetric equation can be applied at any stage of depletion of a reservoir. Before

production data is available, volumetric estimations can be made to calculate GIIP. Volumetric calculations can also be used throughout the production period of a well in comparison to material balance approaches.[10]

The volumetric estimate can be expressed simply by this Equation 2.1.

$$G = \frac{43560 A h \emptyset (1 - S_{wi})}{Bgi} \qquad \text{Eq.II.12}$$

Where:

G is gas in place, scf.

Ø is reservoir porosity, fraction.

h is reservoir thickness, ft.

A is area of reservoir, acres.

Swi is water saturation, fraction.

Bgi is gas formation volume factor at the initial reservoir pressure, ft3/scf.

The gas formation volume factor can be computed by:

$$B_g = Z \frac{T}{P} \frac{P_{sc}}{T_{sc}} \qquad \text{Eq.II.13}$$

Where;

Z is the compressibility factor of gas.

Psc is pressure at standard conditions, psia.

Tsc is temperature at standard conditions, ^{o}F.

II.6.2. Material balance estimation for gas

The material balance technique for calculating gas reserves, like material balance for oil, attempts to mathematically equilibrate changes in reservoir volume as a result of production. The basic equation is

The equations used to calculate OGIP are

Gas reservoir with active water drive:

$$G = \frac{G_p B_g - (W_e - W_p B_w)}{B_g - B_{gi}} \quad \text{Eq.II.14}$$

Gas reservoir with no water drive ($W_e = 0$):

$$G = \frac{G_p B_g + (W_p B_w)}{B_g - B_{gi}} \quad \text{Eq.II.15}$$

Where:

- G = OGIP (SCF)
- G_p = cumulative gas produced (SCF)

These equations can also be used to predict G_p (recoverable reserves) assuming G is determined by an independent method and the production conditions remain constant.

II.6.3. Analogy method

The analogy method for estimating reserves directly compares a newly discovered or poorly defined reservoir to a known reservoir thought to have similar geological or petrophysical properties (depth, lithology, porosity, and so on). While analogy is the least accurate of the methods presented, it is often used early in the life of a reservoir to establish an order-of-magnitude recovery estimate. As the field matures and data become available to make volumetric OGIP estimates, analogy is often used to establish a range of recovery factors to apply to the in-place volumes. Evaluating recovery in this fashion is particularly useful when some performance history is available but a decline rate has yet to be established. Analogy should always be used in conjunction with other techniques to ensure that the results of the more computationally intensive methods make sense within the geological framework.[11]

Chapter III:

Numerical simulation of reservoirs

III.1. Presentation of the regional directorate of Ohanet

III.1.1. Guelta North (GLN) Gas Field Background

III.1.1.1. Geographic location and discovery

Guelta North Field is located in the Illizi Basin (South Eastern part of the Algerian Sahara Desert), at about100 km to the North of In Amenas town (**FigureIII.1**) in the Tinrhert highland (plateau de Tinrhert).

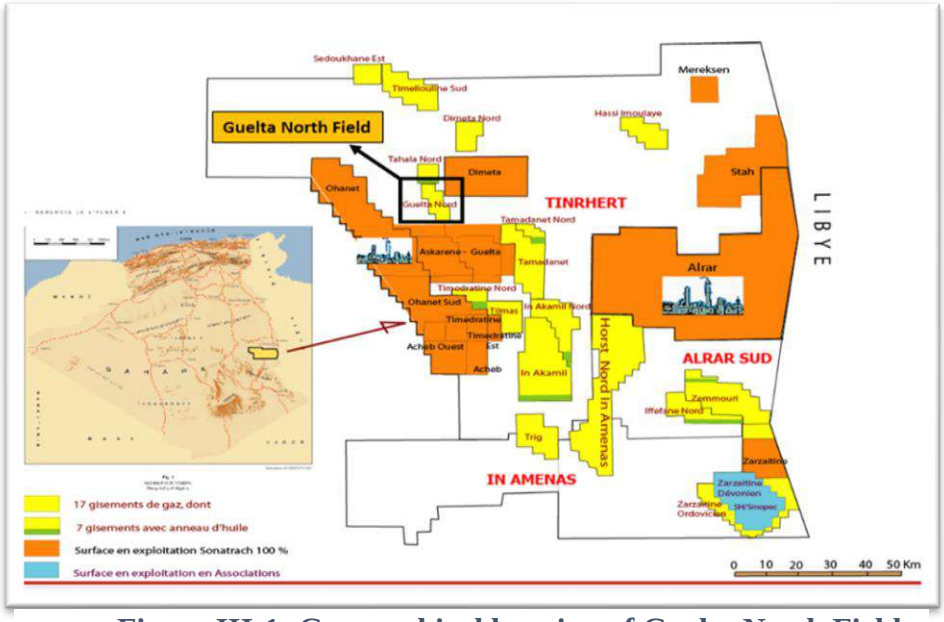

Figure III-1: Geographical location of Guelta North Field

The field was discovered in 2015 after the drilling of well GLN-01 located at the top of the structure. Sweet gas condensate was revealed in the Devonian F2, Siluro-Devonian F6-B&C, and the Ordovician unit IV reservoirs proved by wells GLN-1 to 5 and well THLS-2.

Currently Guelta North field is part of seventeen (17) marginal gas development fields called ‘’Tinrhert gas project’’ with the objective to develop, and produce these fields through ‘’Alrar gas facilities’’ located to the East.

III.1.1.2. Geological and Reservoir Context

III.1.1.2.1. Guelta North Stratigraphy

The **Figure III.2** shows the formations encountered in the drilling of most Guelta North wells which is typical to Illizi Basin penetrations. From stratigraphic stand point, these formations are mainly Paleozoic (Cambrian, Ordovician, Devonian, Carboniferous & Triassic) and Mesozoic (Cretaceous & Jurassic) eras.

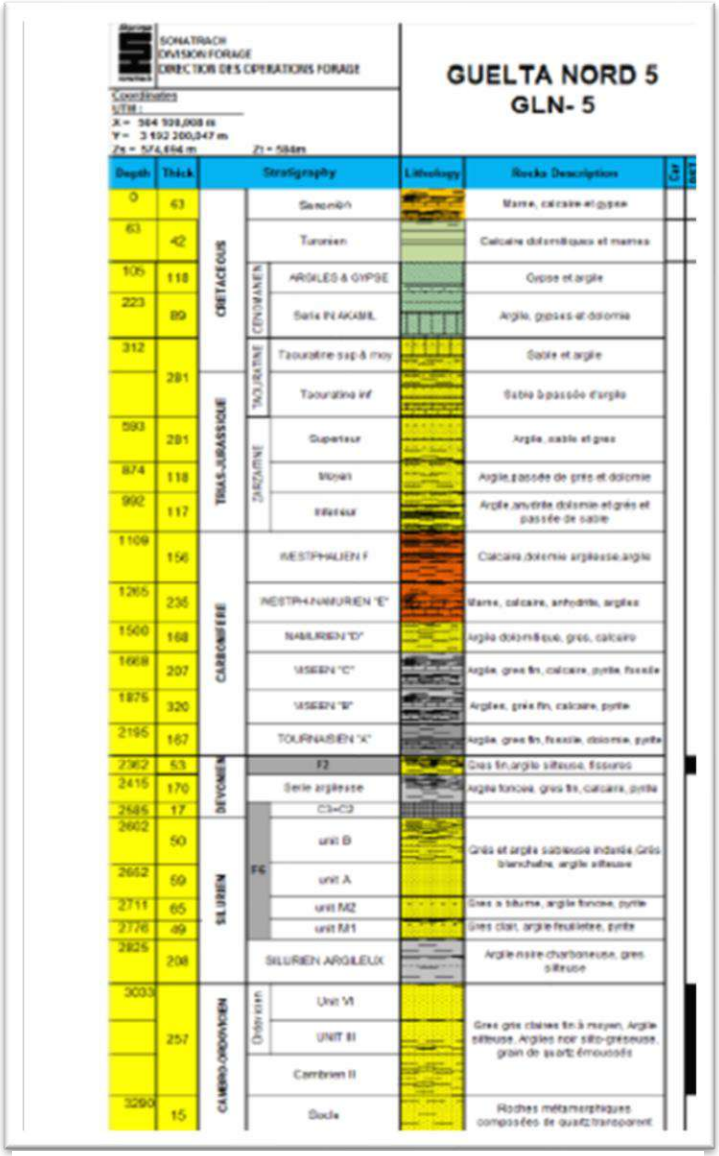

Figure III-2: Guelta North Stratigraphy

III.1.1.2.2. Guelta North Structure

Guelta North structure is a 10 x 7 Km North-West/South-West fault bounded half anticlinal, with xx ft closure (**FigureIII.3**). The structure was delineated and developed with six wells which defined the main structural and stratigraphic elements.

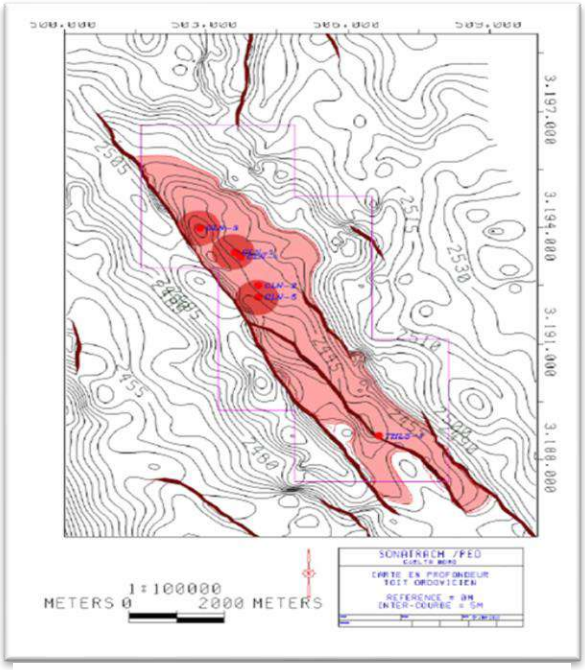

Figure III-3: Guelta North Structure at top Ordovician Unit IV-3 reservoir

III.1.1.2.3. Guelta North Ordovician IV Reservoir

Guelta North produces sweet gas and condensate from the two Ordovician IV-2 and IV-3 shally sandstone units. **Figure IIIIII.4 shows** a typical reservoir log of the Ordovician IV reservoir. The productive reservoir is subdivided in two sub unites; Ordovician IV-3 Unit and Ordovician IV-2 Unit as shown in **Table III.1**

Ordovicien IV-3 Unit

This unit is characterized gray to clear fine to medium Sandstone with thin dark shale laminations

Ordovicien IV-2 Unit

It is predominately dark gray shale sometime silty, with gray to white fine to medium Sandstone intercalation, often quarzitic or carbonate

The table below summarize the main Petro physical properties of the productive Ordovician reservoir in Guelta North Field:

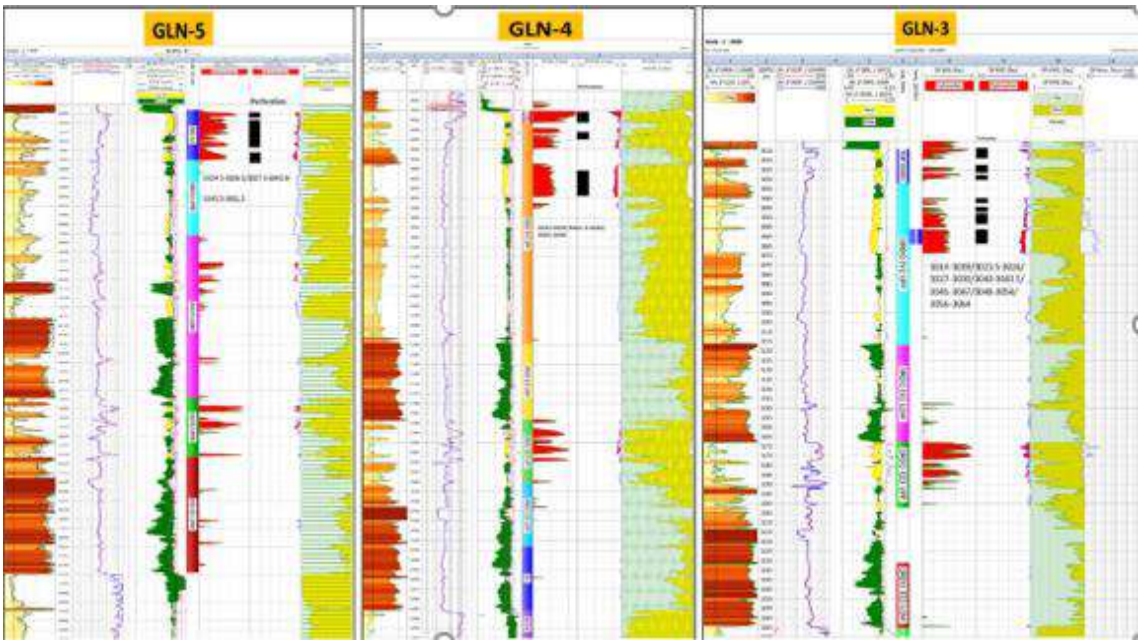

Figure III-4: Guelta North Ordovician IV reservoir interwells correlation

Table III-1: Petro physical properties of the Ordovician reservoir (GLN)

Unit	Thickness (m)	Porosity (%)	Water Saturation (%)	Pay zone (m)
Ordovician IV-3	25	3 to 8		
Ordovician IV-2	130			

The Ordovician IV reservoir was tested in Guelta North Field in three wells; GLN-3, 4 and 5 and produced the following results:

Reservoir pressure was estimated from the Drill Stem Tests (DST) to ~254 kg/cm2 at datum depth –3063 m TVDSS

Reservoir temperature was estimated to **235,4 °F**

The **Table III.2** below summarizes the initial flow test results and PTA (pressure transient analysis) conducted con the three wells GLN-3, 4 and 5:

Table III-2: the initial flow test results and PTA

Well	**Gas Rate (m3/J)**	**Condensate Rate (m3/J)**	**Well Stream CGR (m3/million m3)**	**Kh (md.m)**	**K (md)**	**Skin**	**P* (kg/cm2)**
GLN-3	98756	9.31	94	34	1	1.8	259.7
GLN-4	300251	21.3	71	425	12	5.3	260.1
GLN-5	60420	12	200* (abnormally high)	50	1.1	12.8	259.8

III.2. Numerical simulation of reservoirs

III.2.1. Eclipse 100 simulator

III.2.2. What is Eclipse 100 simulator

ECLIPSE 100 is a fully-implicit, three phase, three-dimensional, general purpose black oil simulator with gas condensate option.

•Program is written in FORTRAN77 and operate on any computer with an ANSI-standard FORTRAN77 compiler and with sufficient memory.

•ECLIPSE 100 can be used to simulate 1, 2 or 3 phase systems. Two phase options (oil/water, oil/gas, gas/water) are solved as two component systems saving both computer storage and computer time. In addition to gas dissolving in oil (variable bubble point pressure or gas/oil ratio), ECLIPSE 100 may also be used to model oil vaporizing in gas (variable dew point pressure or oil/gas ratio).

•Both corner-point and conventional block-center geometry options are available in ECLIPSE. Radial and Cartesian block-center options are available in 1, 2 or 3 dimensions. A 3D radial option completes the circle allowing flow to take place across the 0/360-degree interface.

III.2.3. How to start

- Running simulation needs an input file with all data concerning reservoir and process of its exploitation.
- Input data for ECLIPSE is prepared in free format using a keyword system. Any standard editor may be used to prepare the input file. Alternatively, ECLIPSE Office may be used to prepare data interactively through panels, and submit runs.[26].

III.2.4. Simulation architecture

Once all the data necessary for the simulation are collected and the input files are prepared according to the format required by the simulator, the data is introduced according to a well-defined architecture, this being the subject of this part.

The reservoir modeling strategy is based on two steps:

1) Data collection and synthesis
2) Construction of the simulation model

The database to be integrated into the simulator includes:

- Geological data (static model, skeleton otherwise called the grid).
- Petrophysical data (Permeability, porosity, NTG, initial saturation, fluid contacts).
- Fluid modeling data and rock properties (PVT, rock compressibility, relative permeability, capillary pressure).
- Initialization data.
- Production and pressure data

III.2.5. Description of the Reservoir

The reservoir is a Wet gas reservoir that is 30,000 ft long and 19,200 ft wide. Production history is available from three wells that have been producing for fifteen months. The reservoir average pressure and three observation wells' pressures are also available. The reservoir is surrounded by a finite aquifer. A Cartesian grid system is constructed over the area of the reservoir. 75 grid cells were used in the long direction (30,000 ft) and 98 grid cells were used in the short direction (19,200 ft). The reservoir consists of one zone. Reservoir data is available from the 3 wells that have been drilled in the reservoir. **FigureIII.5:** illustrates the reservoir model generated by use of the Computer Modelling Group (CMG) geostatistical package.

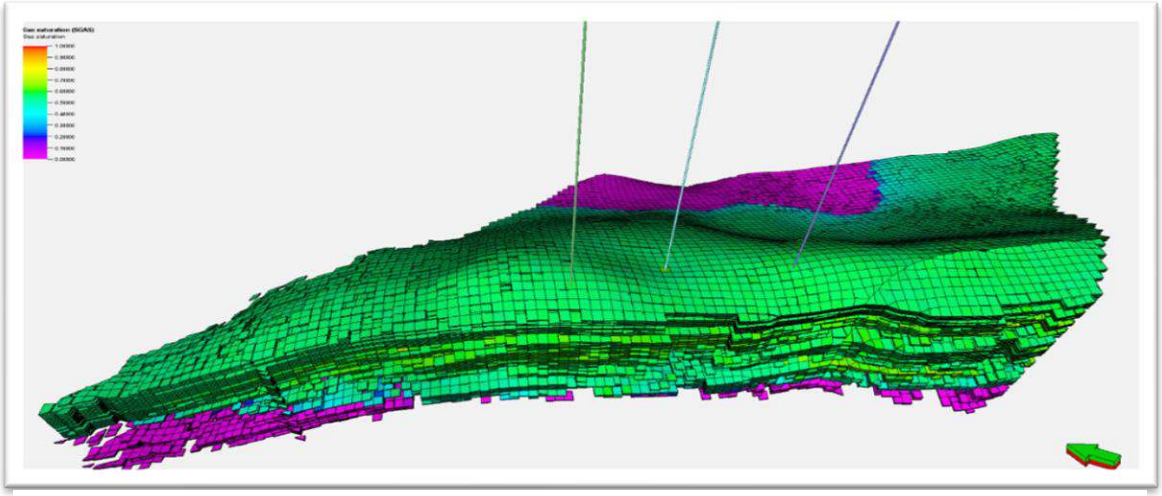

Figure III-5: Hypothetical Reservoir model generated by use of the Computer Modelling Group (CMG) geostatistical package

III.3. Dynamic Model Construction

III.3.1. Initialization data

III.3.1.1. Initial Pressure and Temperature:

A good estimate of the initial pressure of the reservoir is a parameter of major importance for the reliability of the simulation results; in this case the results of **DST** of the first three wells drilled were used (GLN-3, GLN-4 and GLN-5), the pressure average is therefore estimated is **254bar** -2552 (m TVDSS).

The temperature initial is: **235,4 °F**

The initial pressure model is shown in the **Figure III.6** below:

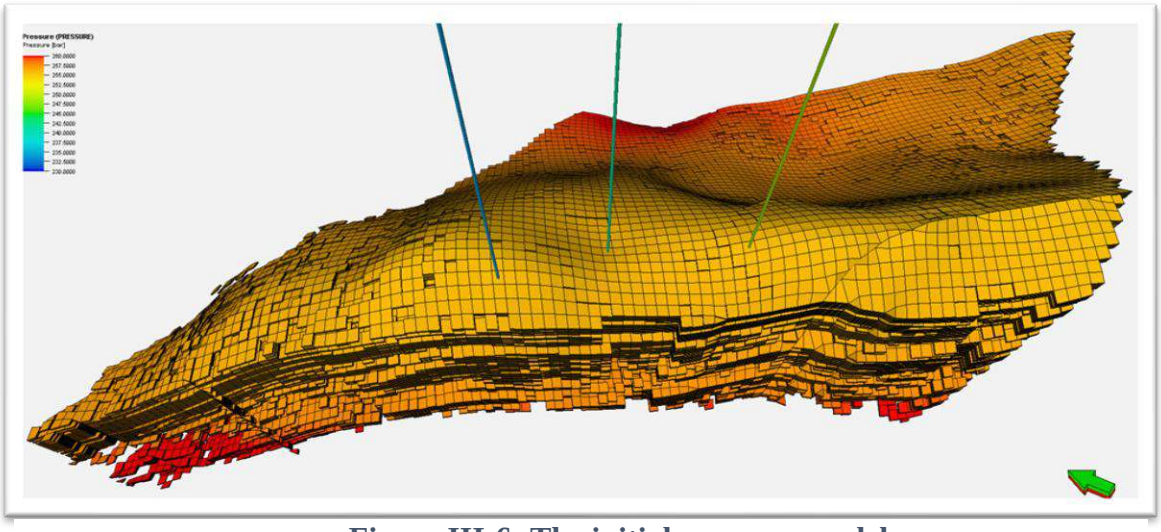

Figure III-6: The initial pressure model

III.3.1.2. Contacts:

The water-gas contact is: 2552 (m TVDSS), the contact was estimated from the petrophysical date (MDT data),

The water-gas contact model is shown in **Figure III.7** below:

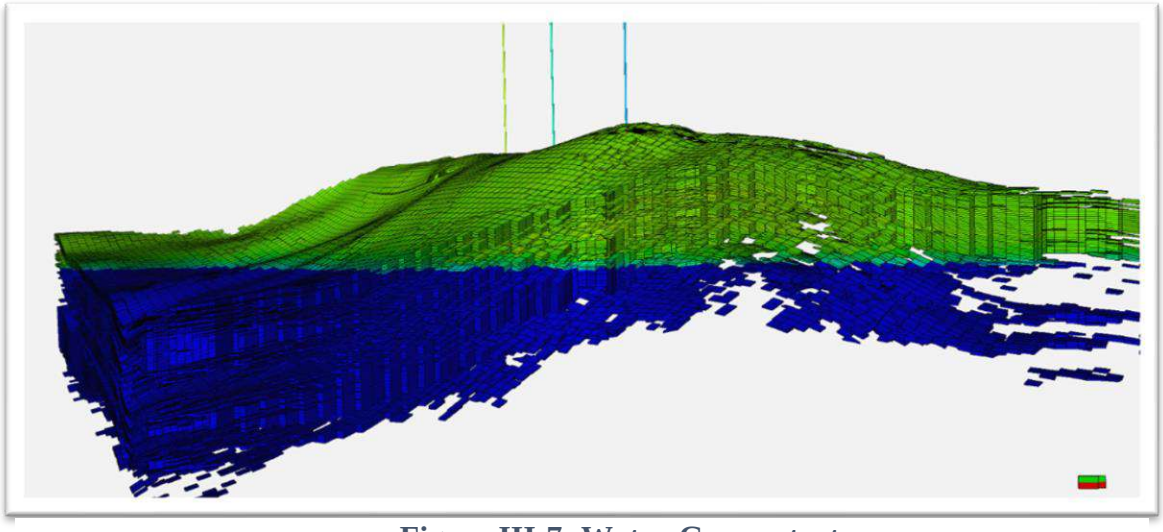

Figure III-7: Water-Gas contact

III.3.2. Rock properties

III.3.2.1. Rock compressibility

Table III-3: Rock compressibility parameter

Field	Reservoir	The reference pressure (Pref) (bar)	The rock compressibility (1/bar)
Guelta-North	Ordevicien unit IV	245.7	7.98E-05

III.3.2.2. Relative Permeabilities

The relative permeability due to a lack of special core analysis (SCAL) data for the relative permeability, the oil - water and gas - relative permeability data were taken from the analogous reservoirs. permeability information of the Ordovician reservoir from the Ohanet field was used for the Ordovician reservoirs in the GLN field. The normalized oil water and gas - divaler relative permeability curves are shown on **Figure III.8.**

Table III-4 Oil-Water Saturation Table

Field	Reservoir	Water saturation (Sw)	Water relative permeability (Krw)	Oil relative permeability (Kro)	Water-Oil capillary pressure (Pcow)
Guelta -No	Ordovicien IV	0	0	1	2.57251
Guelta -N	Ordovicien IV	0.025	0.0000052	0.95063	0.257305
Guelta -N	Ordovicien IV	0.1	0.0005012	0.81	0.066543
Guelta -N	Ordovicien IV	0.65	0.2413315	0.1225	0.002806
Guelta -N	Ordovicien IV	0.75	0.3869922	0.0625	0.002011
Guelta -N	Ordovicien IV	0.775	0.4312167	0.05062	0.001859
Guelta -N	Ordovicien IV	0.8	0.4788472	0.04	0.001721
Guelta -N	Ordovicien IV	0.875	0.6436156	0.01562	0.001379
Guelta -N	Ordovicien IV	0.975	0.9198462	0.00062	0.001046
Guelta -N	Ordovicien IV	1	1	0	0.000979

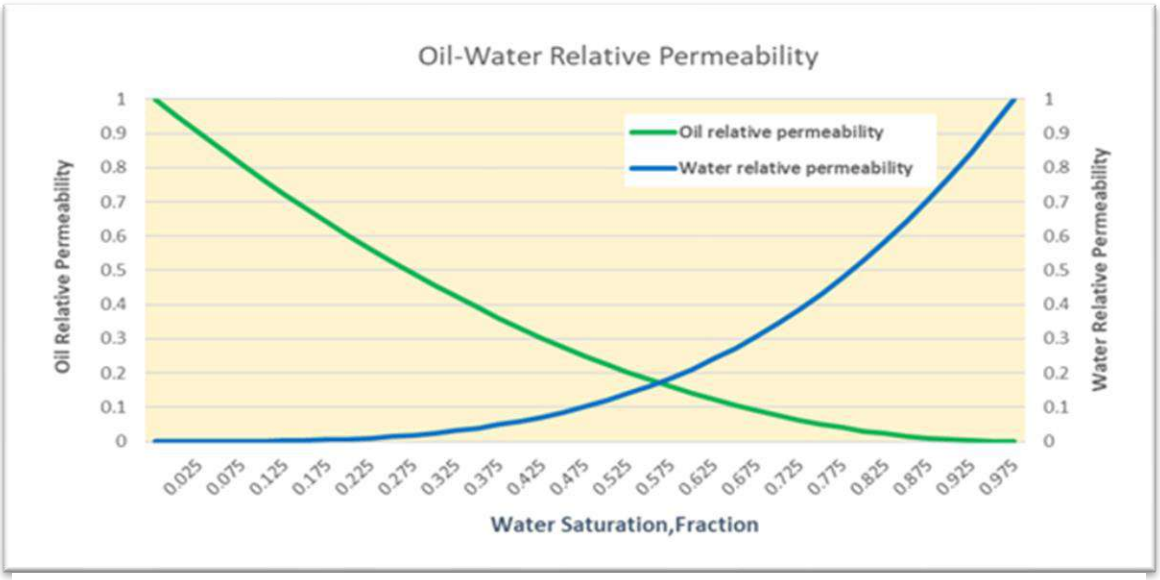

Figure III-8: Oil-water relative permeability

Field	Reservoir	Gas Saturation (Sg)	Gas Relative Permeability (Krg)	Krog
Guelta-North	Ordevicien IV	0	0	1
Guelta-North	Ordevicien IV	0.025	0.001307	0.95063
Guelta-North	Ordevicien IV	0.1	0.0158489	0.81
Guelta-North	Ordevicien IV	0.125	0.0236831	0.76563
Guelta-North	Ordevicien IV	0.2	0.0551892	0.64
Guelta-North	Ordevicien IV	0.3	0.1145034	0.49
Guelta-North	Ordevicien IV	0.425	0.2143384	0.33063
Guelta-North	Ordevicien IV	0.525	0.3135355	0.22563
Guelta-North	Ordevicien IV	0.625	0.4291252	0.14063
Guelta-North	Ordevicien IV	0.7	0.5262311	0.09
Guelta-North	Ordevicien IV	0.725	0.5605423	0.07562
Guelta-North	Ordevicien IV	0.775	0.6320378	0.05062
Guelta-North	Ordevicien IV	0.825	0.7073219	0.03062
Guelta-North	Ordevicien IV	0.9	0.8272495	0.01
Guelta-North	Ordevicien IV	0.95	0.9118061	0.0025
Guelta-North	Ordevicien IV	1	1	0

III.3.3. Fluid properties:

III.3.3.1. Gas properties:

There was no fluid PVT report available for the Ordovician reservoirs in the GLN study field. A black-oil approach was used to model the properties of the field in GLN field. The variations of fluid PVT properties with pressure were estimated from the fluid PVT properties available in the provided DST reports using applicable fluid PVT correlations available in literature. The estimated variations with pressure for the reservoir gas formation volume factor and gas viscosity are shown on **FigureIII.9**,

The PVTG table input of model is shown in the table below:

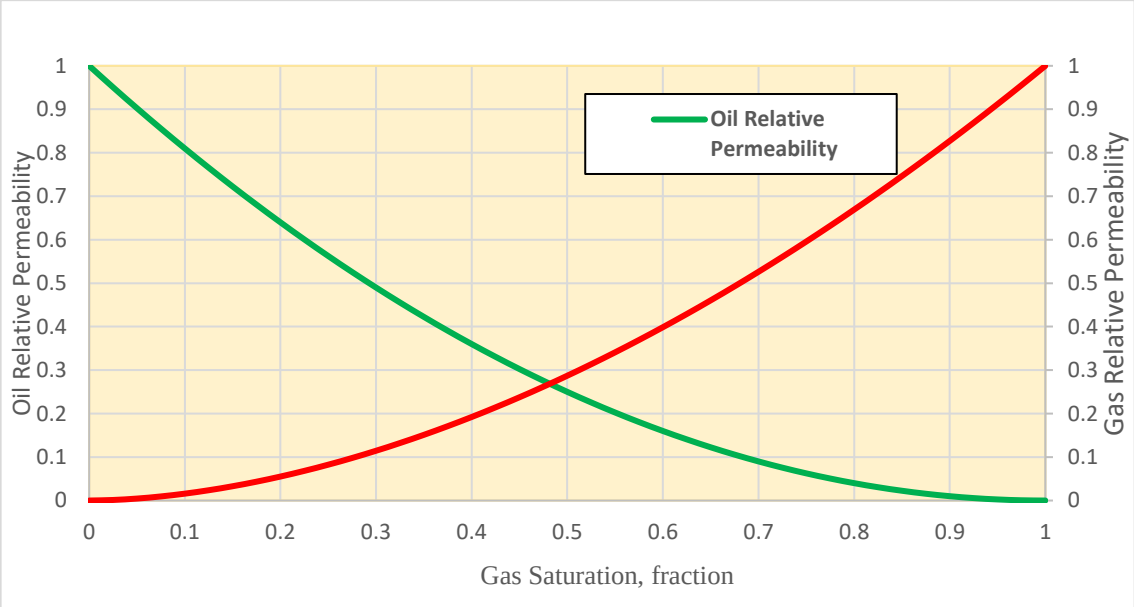

Figure III-9: Oil-Gas Relative Permeabilities

Table III-4 The PVTG table input of model

Field	Reservoir	The gas phase pressure (Pg)	Compressibility (1/psi)	Viscosity (cP)
Guelta-North	Ordevicien IV	**413.42**	**0.0033**	**0.0316**
Guelta-North	Ordevicien IV	**265.1**	**0.0047**	**0.0234**
Guelta-North	Ordevicien IV	**240.09**	**0.0051**	**0.022**
Guelta-North	Ordevicien IV	**206.84**	**0.0058**	**0.0202**
Guelta-North	Ordevicien IV	**172.37**	**0.0069**	**0.0184**
Guelta-North	Ordevicien IV	**137.9**	**0.0086**	**0.0168**
Guelta-North	Ordevicien IV	**68.95**	**0.018**	**0.0145**
Guelta-North	Ordevicien IV	**34.47**	**0.0372**	**0.0138**

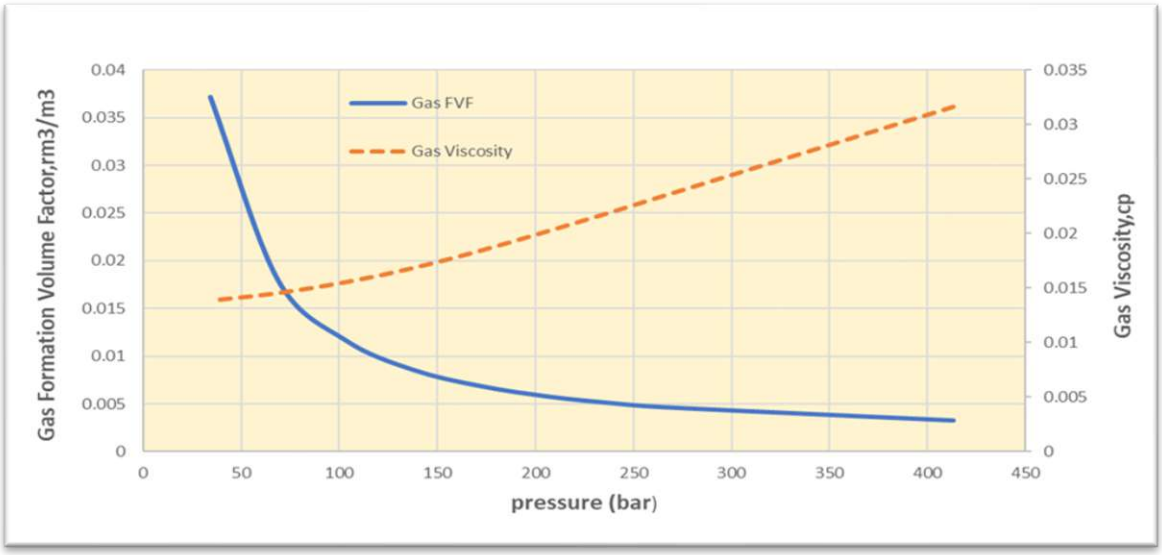

Figure III-10: Gas viscosity and volume factor

III.3.3.2. Water properties:

Table III-5 Water properties table

Field	Reservoir	FVF (bbl/STB)	Compressibility (1/psi)	Viscosity (cP)
Guelta-North	Ordevicien IV	1.036	3.93E-05	0.319

III.3.4. The static model outputs:

III.3.4.1. Porosity model:

The porosity data from the cored sections of the wells were used to make a stochastic distribution of the porosity in the whole reservoir using the algorithm sequential Gaussian simulation (SGS).

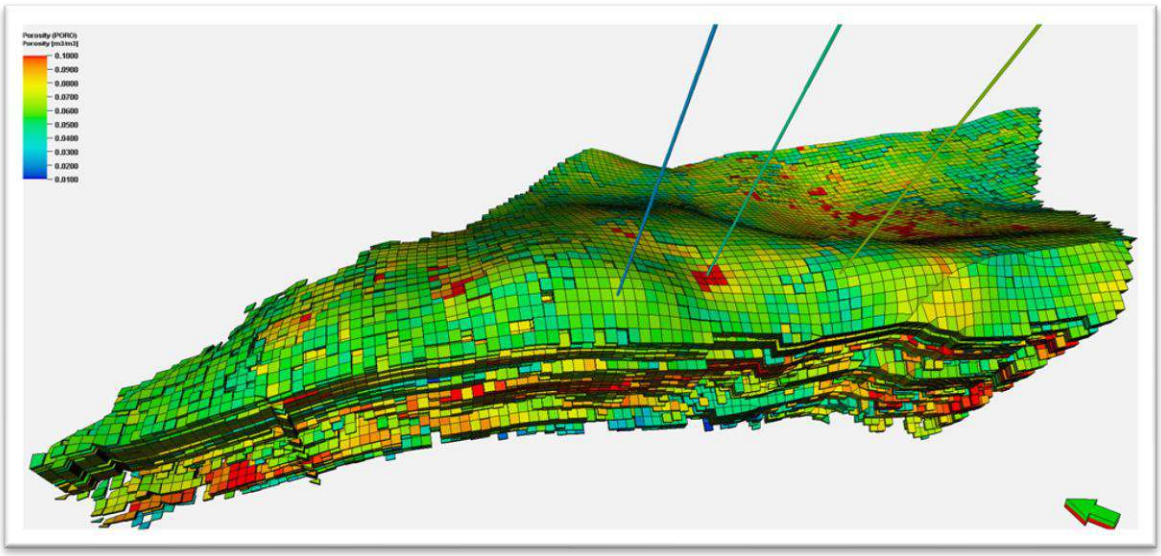

Figure III-11: Model show the permeability distribution in the Guelta-North field

III.3.4.2. Permeability model:

Once the distribution of rock type and porosity is made relationships porosity-permeability "equations" have been established according to the rock type.

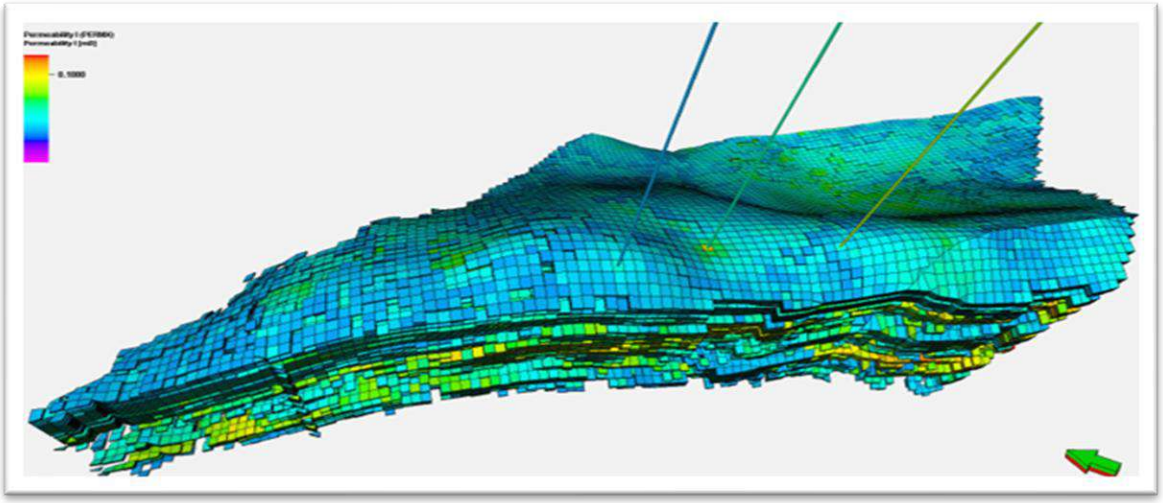

Figure III-12: Model show the permeability distribution in the Guelta-North field

III.3.4.3. Faults model

Faults picked from the 3D seismic data, incorporated in the static model.

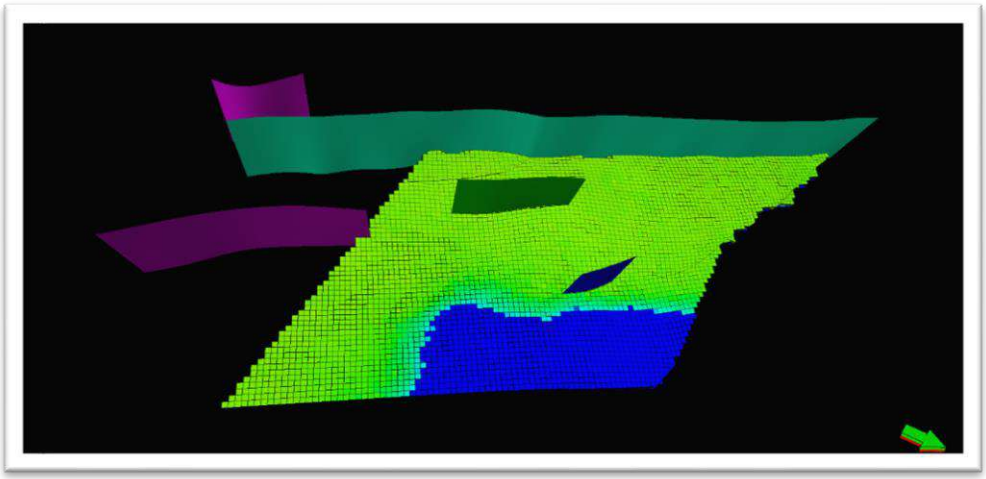

Figure III-13: Guelta North Fault model in 3D

III.3.4.4. Model of the initial water saturation:

The modeling of the initial water saturation is essential for the calculation of the reservation; it is based on the function J defined below

For each type of rock, we have:

$$J(s_w) = 0.2166 * \frac{Pc}{\sigma \cos\theta} * \sqrt{\frac{k}{\phi}} \qquad \text{Eq.III.01}$$

$$J(S_w) = \frac{(S_w - B)^{(-1/\lambda)}}{A} \qquad \text{Eq.III.02}$$

Where:

$$S_w = AJ^{-\lambda} + B \qquad \text{Eq.III.03}$$

A and λ are coefficients determined by regression

B: irreducible water saturation for each rock type

J: Levertt function

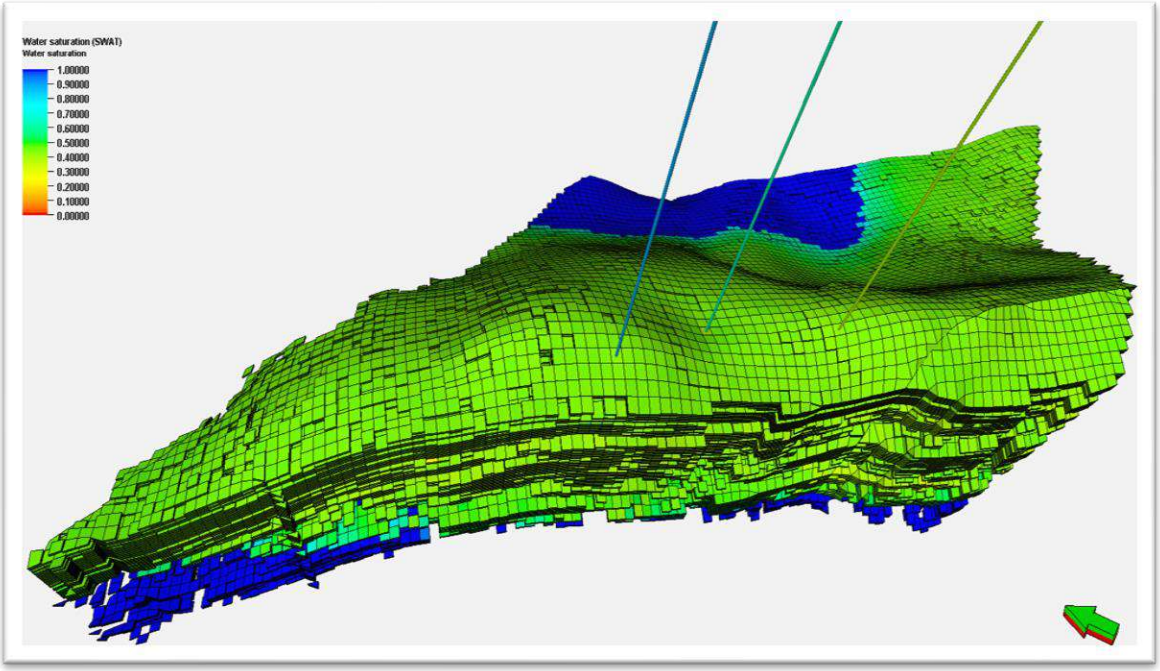

Figure III-14: Model show the water saturation in the Guelta-North field

III.3.5. Guelta North production history

Guelta North gas field was put on stream in Nov 2020 from three wells GLN-3, 4 and. The field cumulative gas production after 14 months (December 2021) is XXX million Stm3.

The **Figure III.15** and **Table III.3** display daily and cumulative gas production up to December 2021

Table III-6 gas production of the field

Field	Reservoir	Status	Date	Field gas rate (sm3/d)	Monthly Production (sm3)	Cumulative production (sm3)	Recovery factor (%)
Guelta - North	Ordovicien IV	GP	01-Nov-20	1540.9836	47000	47000	0.0000060880
Guelta - North	Ordovicien IV	GP	01-Jan-21	18644.269	568650.2	1167648	0.0001512 5
Guelta - North	Ordovicien IV	GP	01-Feb-21	14978.721	456851	1624499	0.0002104 27
Guelta - North	Ordovicien IV	GP	01-May-21	16525.646	504032.2	3131688	0.0004056 59
Guelta - North	Ordovicien IV	GP	01-Sep-21	16417.367	500729.7	4649089	0.0006022 14
Guelta - North	Ordovicien IV	GP	01-Dec-21	14955.574	456145	6047571	0.0007833 64

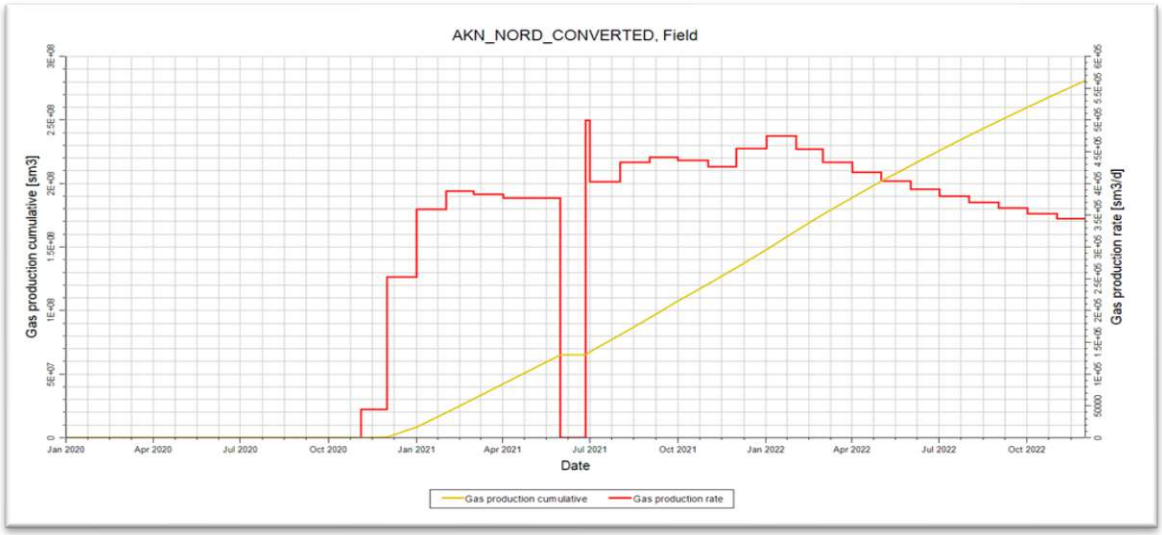

Figure III-16: Gas production cumulated/rate curve

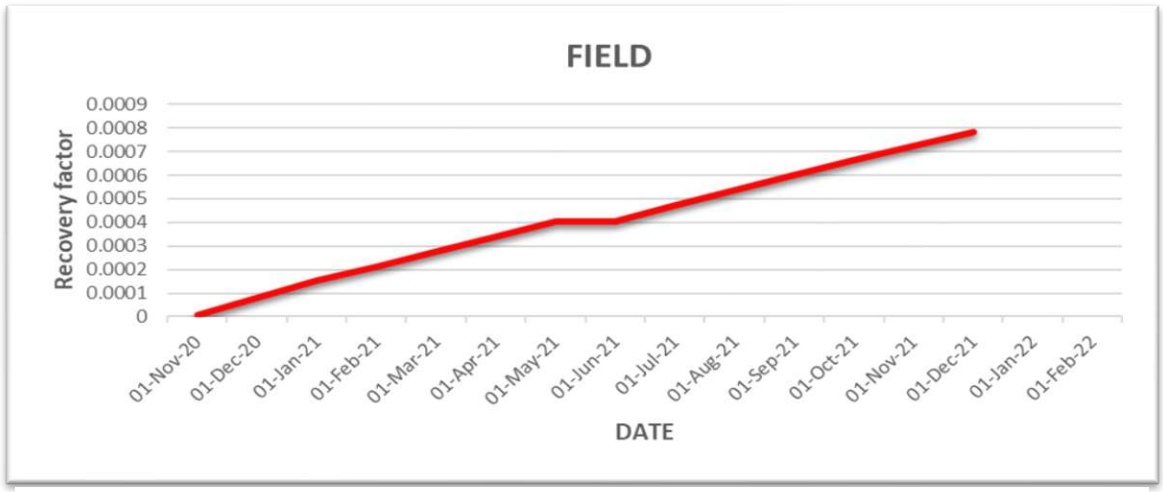

Figure III-15: Gas production curve recovery factor

The average daily production of the field is 14754 sm3/d. After fourteen months of production, cumulative production reached 6.05 Msm3 in December 2021.

The tables and graphs below show the production and the tubing head pressure per well:

Table III-7 gas production of the well GLN-3

Date	Gas rate (sm3/d)	Monthly Production (sm3)	Cumulative production (sm3)	Tubing head pressure (bar)	Observations
01-Dec20	2868.764	87497.3	87497.3	109	
01-Jan-21	2831.265	86353.59	173850.9	102	
01-Feb21	2755.269	84035.71	257886.6	95	
01-Mar21	2755.156	84032.25	341918.9	95	
01-Apr-21	2837.965	86557.93	428476.8	91	
01-May-21	2755.156	84032.25	512509	91	
01-Jun-21	0	0	512509	0	Station problem
01-Jul-21	2815.709	85879.12	598388.2	89	
01-Aug-21	2760.444	84193.54	682581.7	84	
01-Sep-21	2738.115	83512.5	766094.2	79	
01-Oct-21	2411.633	73554.8	839649	75	
01-Nov-21	2018.595	61567.16	901216.2	72	
01-Dec-21	1842.536	56197.34	957413.5	81	

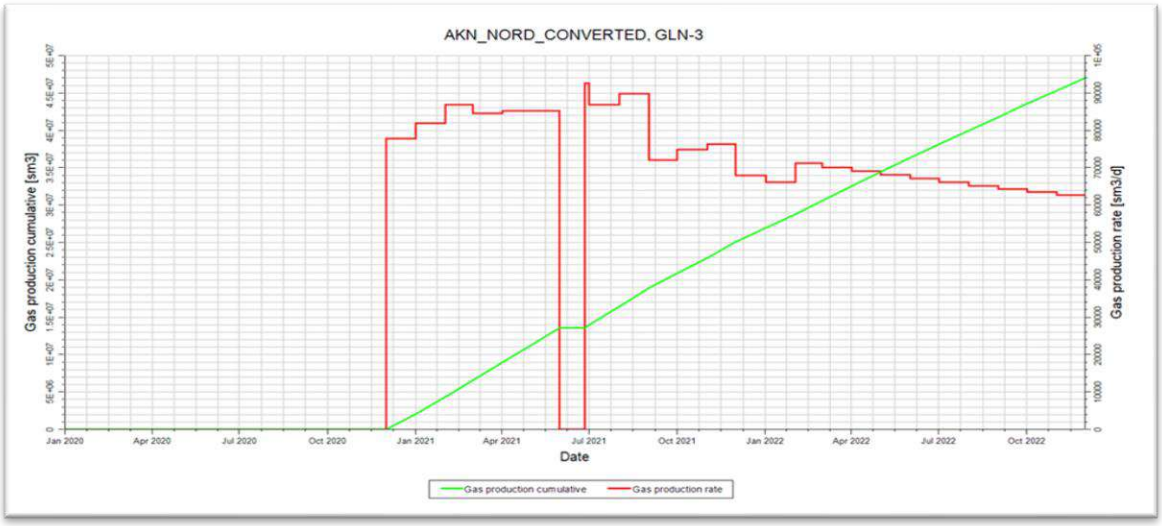

Figure III-18: GLN-3 Gas production cumulated/rate curve

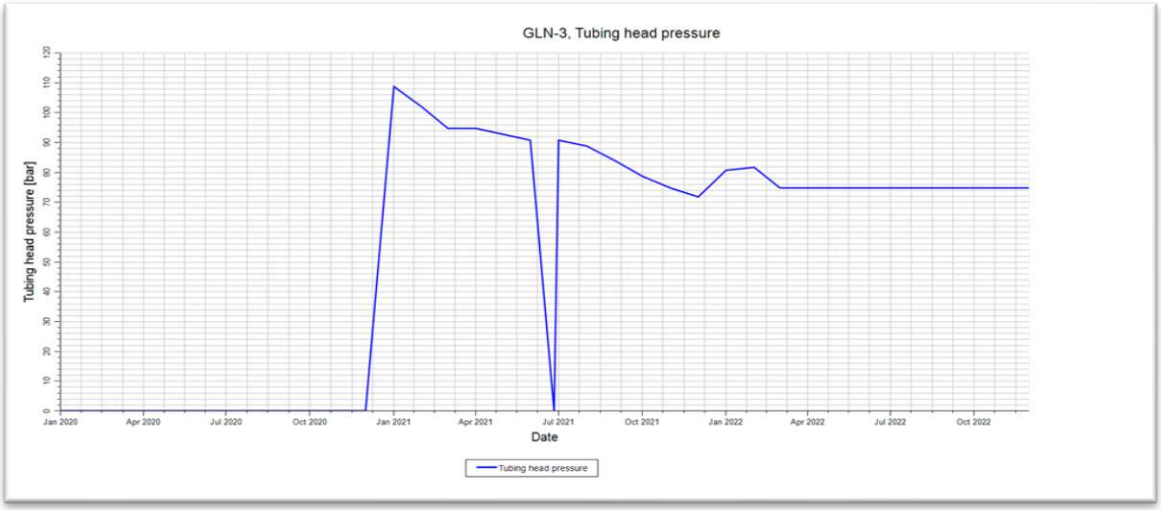

Figure III-17: GLN-3 Tubing Head pressure

Table III-8 GLN-4 well gas production

Date	Gas rate (sm3/d)	Monthly Production(sm3)	Cumulative production(sm3)	Tubing head pressure (bar)	Observations
01-Dec-20	13605.4	414964.6	414964.6	166	
01-Jan-21	14188.86	432760.3	847724.9	148	
01-Feb-21	10656.71	325029.5	1172754	140	
01-Mar-21	12316.23	375645.2	1548400	135	
01-Apr-21	11945.12	364326.2	1912726	129	
01-May-21	12240.08	373322.6	2286048	126	
01-Jun-21	0	0	2286048	0	Station problem
01-Jul-21	12366.57	377180.3	2663229	124	
01-Aug-21	12317.29	375677.4	3038906	116	
01-Sep-21	12186.89	371700	3410606	108	
01-Oct-21	12125.86	369838.7	3780445	105	
01-Nov-21	11356.28	346366.7	4126811	102	
01-Dec-21	11928.08	363806.5	4490618	94	

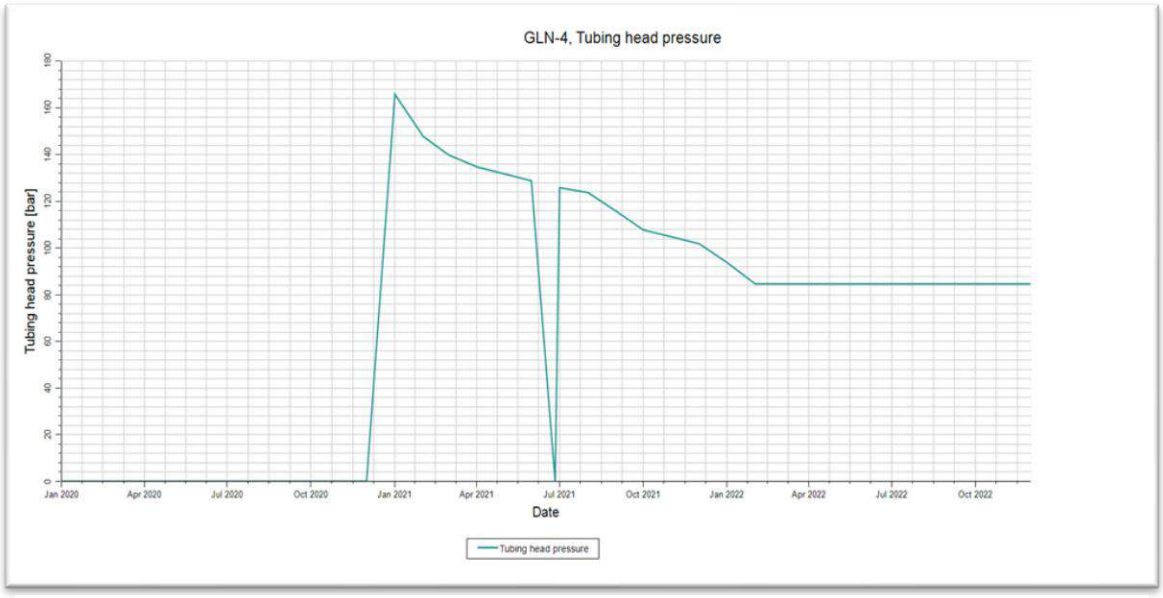

Figure III-20: GLN-4 Tubing Head pressure

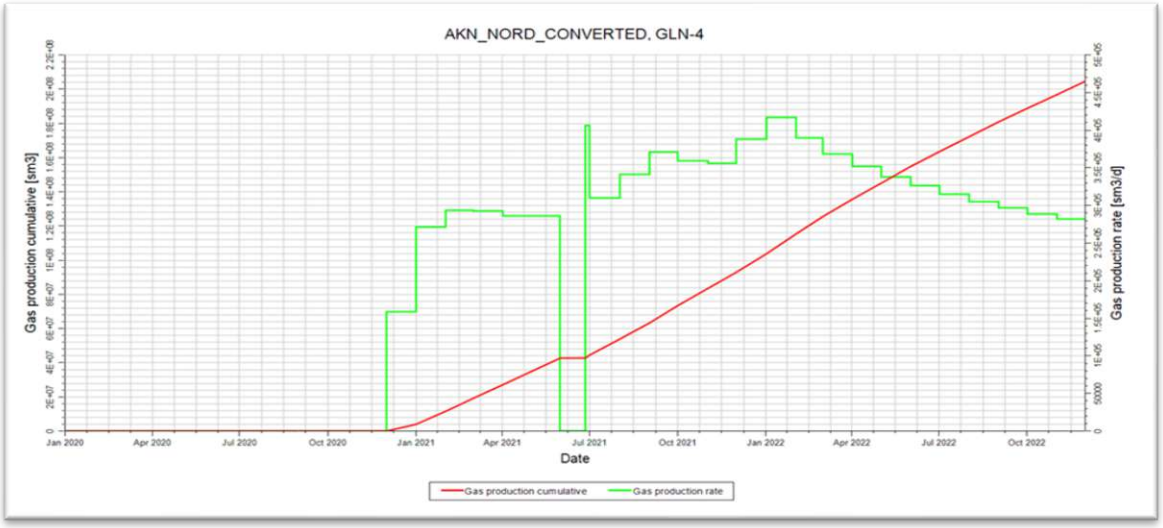

Figure III-19: GLN-4 Gas production cumulated/rate curve

Table III-9 GLN-5 well gas production

Date	Gas rate (sm3/d)	Monthly Production(sm3)	Cumulative production(sm3)	T-head pressure (bar)	Observations
01-Nov20	1661.786	50684.47	c	96	
01-Dec-20	1624.14	49536.27	100220.7	102	
01-Jan-21	1624.14	49536.27	149757	96	
01-Feb-21	1566.745	47785.71	197542.7	86	
01-Mar-21	1542.041	47032.25	244575	88	
01-Apr-21	1493.844	45562.23	290137.2	85	
01-May-21	1530.407	46677.41	336814.6	83	
01-Jun-21	0	0	336814.6	0	Station problem
01-Jul-21	1541.521	47016.39	383831	81	
01-Aug-21	1531.951	46724.51	430555.5	78	
01-Sep-21	1492.369	45517.24	476072.8	76	
01-Oct-21	1520.34	46370.37	522443.1	70	
01-Nov-21	1463.616	44640.28	567083.4	84	
01-Dec-21	1184.956	361416.17	603224.6	69	

Wells trajectories and perforations:

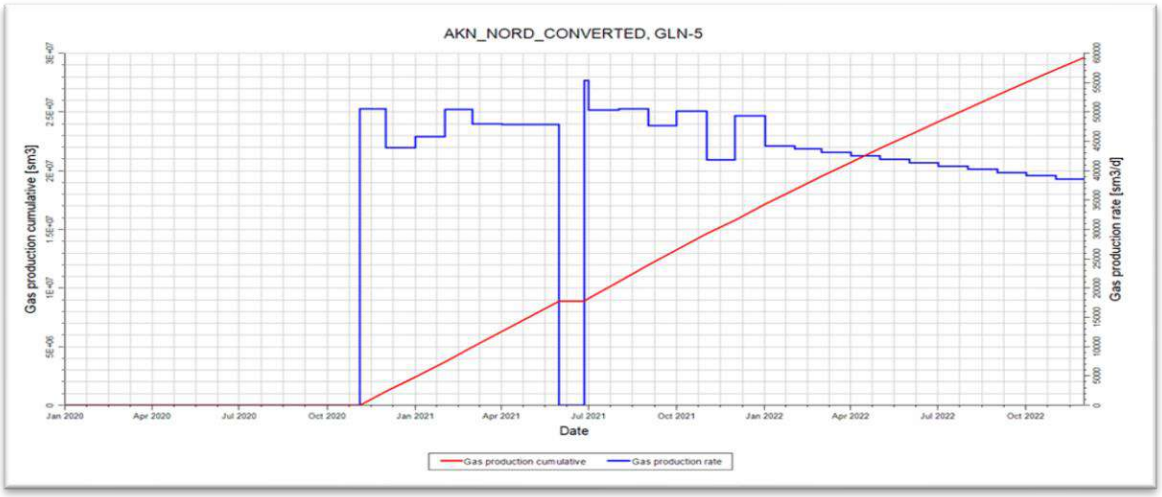

Figure III-22: Gas production cumulated/rate curve

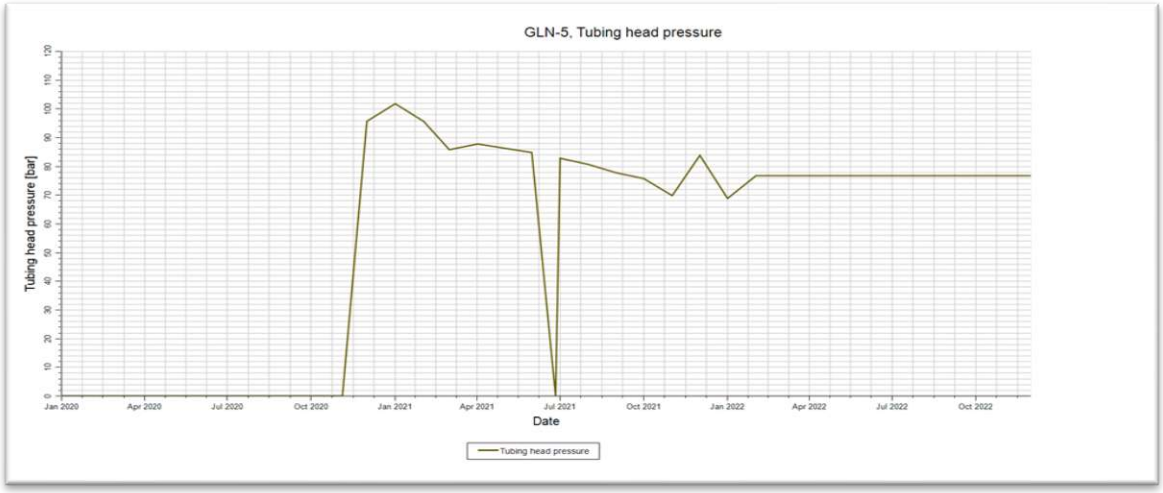

Figure III-21: GLN-5 Tubing Head pressure

The Guelta-North field contain three vertical producers' wells, they producing from the Ordevicien IV

Table III-10 well perforations

Field	Reservoir	Status	Well	Zt (m)	Zs (m)	Depth (mTVDSS)	Perforations (mTVDSS)	
Guelta-North	Ordovicien IV	WGP	GLN-3	575.694	566.394	2714	Top	Bottom
Guelta -N	Ordovicien IV	WGP	GLN-3				2438.306	2443.306
Guelta -N	Ordovicien IV	WGP	GLN-3				2447.80	2450.306
Guelta -N	Ordovicien IV	WGP	GLN-3				2451.306	2454.306
Guelta -N	Ordovicien IV	WGP	GLN-3				2464.306	2467.806
Guelta -N	Ordovicien IV	WGP	GLN-3				2469.306	2471.306
Guelta -N	Ordovicien IV	WGP	GLN-3				2472.306	2478.306

Guelta -N	Ordovicien IV	WGP	GLN-3				2480.306	2488.306
Guelta -N	Ordovicien IV	WGP	GLN-4	581.48	572.16	2724	2449.52	2454.52
Guelta -N	Ordovicien IV	WGP	GLN-4				2461.02	2464.52
Guelta -N	Ordovicien IV	WGP	GLN-4				2480.52	2488.52
Guelta -N	Ordovicien IV	WGP	GLN-5	584.48	574.69	2729	2440	2442
Guelta -N	Ordovicien IV	WGP	GLN-5				2443	2459
Guelta -N	Ordovicien IV	WGP	GLN-5				2461	2467

III.4. History matching

History matching is an iterative process that makes it possible to integrate reservoir geoscience and engineering data. History matching is also referred to as model calibration in the literature because the modeling team should verify and refine the reservoir description during the history match, or model calibration, process. Starting with an initial reservoir description, the model is used to match and predict reservoir performance. If necessary, the modeling team will modify the reservoir description until an acceptable match is obtained.

The history matching process may be considered an inverse problem because an answer already exists. We know how the reservoir performed; we want to understand why. Our task is to find the set of reservoir parameters that minimizes the difference between the model performance and the historical performance of the field. This is a non-unique problem since there is usually more than one way to match the available data.

Description of History Data Available

The following history data is available for the production wells (GLN-3, GLN-4, GLN-5) for fourteen months:

Gas Production Rate (Sm3/D)

Flowing Tubing head Pressure, THP (bar)

III.4.1. Model stability checks:

In dynamic systems analysis, we can define a stable system as one that remains unchanged (or only slightly changed) in the presence of perturbations. Simply put, a stable system is robust to external changes. One way to measure the stability of the reservoir model is by checking the Pressure, (Run model with closed wells, and check pressure stability on 5-10 years).

III.4.2. History match cases:

III.4.2.1. The base case results:

Presentation of the results of the simulation of the base case of the GUELTA-north reservoir:

Once the data file has been prepared, the model is simulated. In the base case we will display and interpret the raw results given by the simulator, this being essential to decide later on the modifications to be made to make the setting.

The volumes in place:

The hydrocarbons initially in place (HIIP) for the low Case, Best case, and High case for the GLN study field was estimated as presented in the following table:

Table III-11GLN field estimated production

		Low case		Base case		High case	
Study Field	**Reservoir**	**Gas (10^9m^3)**	**Condensate (10^6m^3)**	**Gas (10^9m^3)**	**Condensate (10^6m^3)**	**Gas (10^9m^3)**	**Condensate(10^6m^3)**
GLN	Unit IV	6.52	0.43	7.72	0.52	10.87	0.73

The Best technical Case was used to simulate a conceptual development plan using the primary recovery for the GLN study field. The study estimated gas and condensate recovery factor of 44 percent for the Unit IV reservoir of the GLN study field that was estimated to contain wet gas.

The results given by the simulator are*:*

OGIIP= $7.72.10^9 Sm^3$

HCPV= 155441678 Rm^3

```
                                                  ==================================================
                                                  :               FIELD TOTALS                     :
                                                  :         PAV =        256.89  BARSA             :
                                                  :         PORV=    152741678.   RM3               :
                                                  :(PRESSURE IS WEIGHTED BY HYDROCARBON PORE VOLUME:
                                                  : PORE VOLUMES ARE TAKEN AT REFERENCE CONDITIONS):
                        :--------------- OIL    SM3  ---------------:-- WAT    SM3  -:---------------- GAS    SM3  ----------------:
                        :     LIQUID          VAPOUR          TOTAL   :       TOTAL    :       FREE      DISSOLVED          TOTAL   :
:-----------------------:-------------------------------------------:----------------:-----------------------------------------------:
:CURRENTLY IN PLACE     :            0.       510398.        510398.:     114743764. :   7722743446.            0.    7722743446.:
:-----------------------:-------------------------------------------:----------------:-----------------------------------------------:
:OUTFLOW THROUGH WELLS  :                                        0.:            0. :                                          0.:
:WELL  MATERIAL BAL. ERROR:                                      0.:            0. :                                          0.:
:FIELD MATERIAL BAL. ERROR:                                      0.:            0. :                                          0.:
:-----------------------:-------------------------------------------:----------------:-----------------------------------------------:
:ORIGINALLY IN PLACE    :            0.       510398.        510398.:     114743764. :  7722743446.            0.    7722743446.:
=================================================================================================================================================


                                                  ====================================
                                                  :  FIPNUM OIL RECOVERY FACTORS     :
:---------:-----------------------------:-------------------------------------------:-----------------------------------------------:
:         :                             : RATIO OF       RATIO OF       RATIO OF    : RATIO OF       RATIO OF       RATIO OF     :
: REGION  : MOBILE OIIP    MOBILE OIIP  : DISPLACED OIL  DISPLACED OIL  DISPLACED OIL : WELL FLOW      WELL FLOW      WELL FLOW    :
:         : (W.R.T WATER)  (W.R.T GAS)  : TO INITIAL     TO INITIAL     TO INITIAL  : TO INITIAL     TO INITIAL     TO INITIAL   :
:         :                             : OIP            MOBILE OIL     MOBILE OIL  : OIP            MOBILE OIL     MOBILE OIL   :
:         :                             :                (WATER)        (GAS)       :                (WATER)        (GAS)        :
:---------:-----------------------------:-------------------------------------------:-----------------------------------------------:
:   FIELD :    0.000E+00      5.104E+05 :   0.00000                    0.00000      :         0                                    0    :
=================================================================================================================================================
```

Figure III-23: The results are extracted from the PRT file

The graphs below show the results between the production observed and the production modelled of the three wells and the field (case do nothing):

The results of each well:

GLN-3:

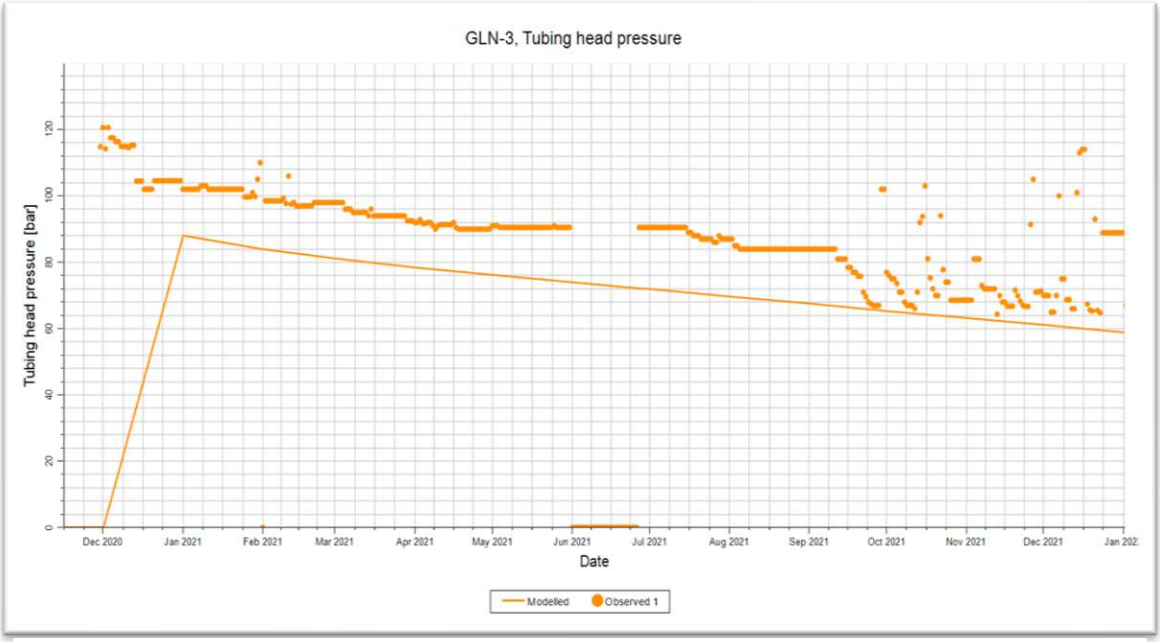

Figure III-25: GLN-3 Tubing Head pressure

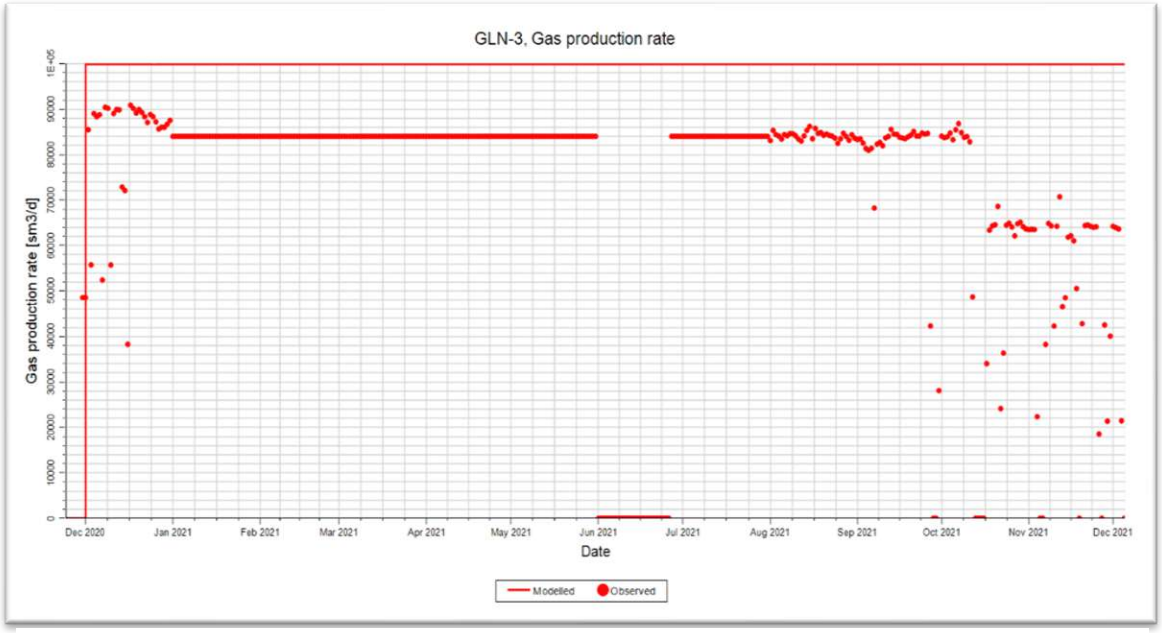

Figure III-24: GLN-3 Gas production rate

GLN-4:

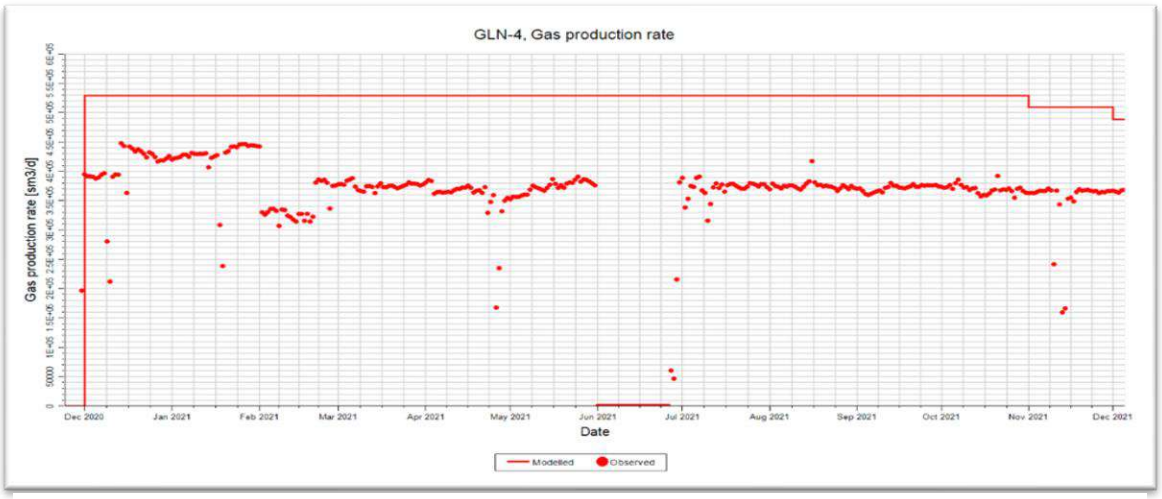

Figure III-27: GLN-4 Gas production rate

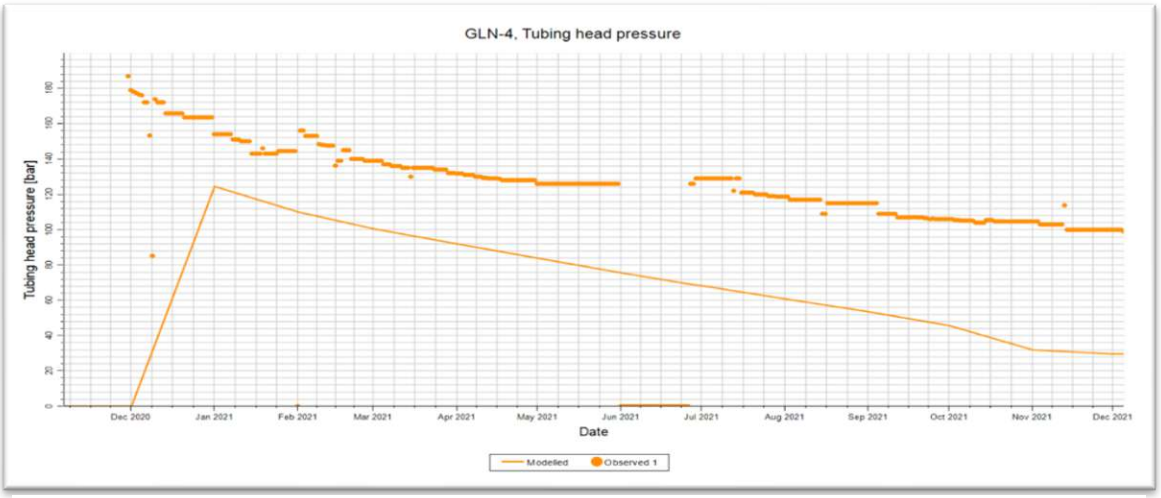

Figure III-26: GLN-4 Tubing Head pressure

GLN 5

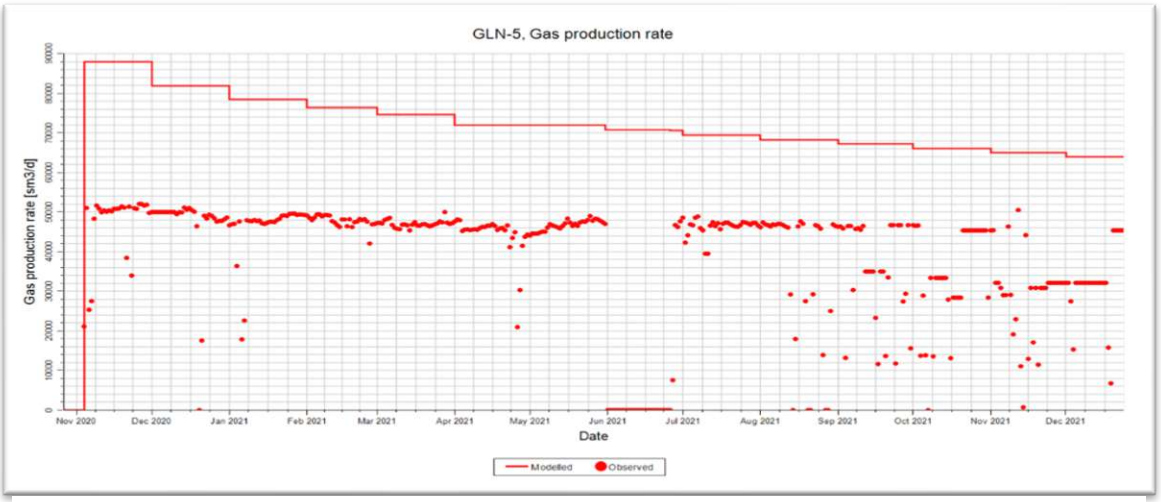

Figure III-28: GLN-5 Gas production rate

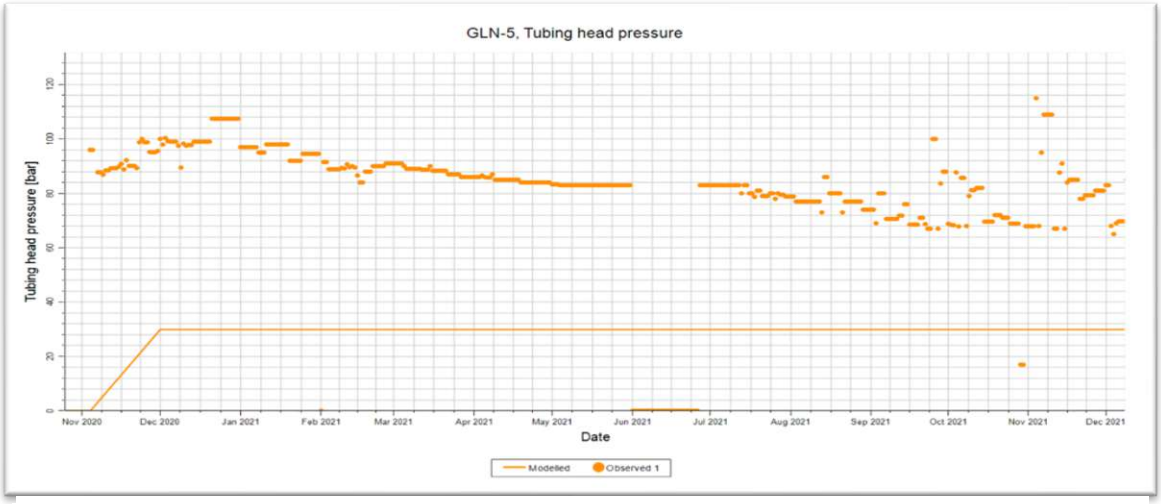

Figure III-29: GLN-5 Tubing Head pressure

Field:

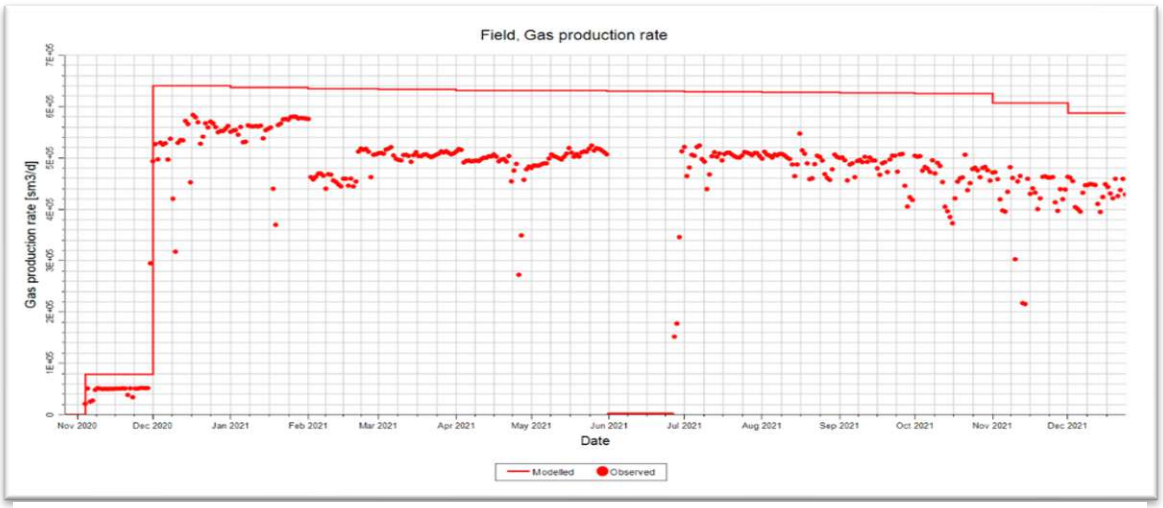

Figure III-30: Global field Gas production rate

III.4.2.2. The Final case

The volumes in place

The results given by the simulator are:

OGIIP= $7.76.10^{9} Sm^{3}$

HCPV= 155441678 Rm^{3}

```
                                                  ==================================================
                                                  :               FIELD TOTALS                     :
                                                  :         PAV =        256.89  BARSA             :
                                                  :         PORV=    155441678.   RM3               :
                                                  :(PRESSURE IS WEIGHTED BY HYDROCARBON PORE VOLUME:
                                                  : PORE VOLUMES ARE TAKEN AT REFERENCE CONDITIONS):
                          :--------------- OIL    SM3  ---------------:-- WAT    SM3  -:--------------- GAS    SM3  ---------------:
                          :     LIQUID         VAPOUR          TOTAL   :       TOTAL    :       FREE      DISSOLVED          TOTAL   :
:-------------------------:-------------------------------------------:----------------:-----------------------------------------------:
:CURRENTLY IN PLACE       :           0.       510398.        510398.:     114743764. :   7652143946.           0.    7652143946.:
:-------------------------:-------------------------------------------:----------------:-----------------------------------------------:
:OUTFLOW THROUGH WELLS    :                                        0.:            0. :                                          0.:
:WELL  MATERIAL BAL. ERROR:                                        0.:            0. :                                          0.:
:FIELD MATERIAL BAL. ERROR:                                        0.:            0. :                                          0.:
:-------------------------:-------------------------------------------:----------------:-----------------------------------------------:
:ORIGINALLY IN PLACE      :           0.       510398.        510398.:     114743764. :   7652143946.           0.    7652143946.:
=============================================================================================================================================


                                          ============================================
                                          : FIPNUM REGION AVERAGED GRID QUANTITIES   :
                                          :        ( WEIGHTED BY PORE VOLUMES        :
                                          :          AT REFERENCE CONDITIONS )       :
:----------:-------------:-------------:-------------:-------------:-------------:
:  REGION  :     PERMX   :     PERMY   :     PERMZ   :      PORO   :      DZ     :
:----------:-------------:-------------:-------------:-------------:-------------:
:   FIELD  :      0.062  :      0.062  : 6.2486E-04  :    0.08002  :       1.08  :
=============================================================================================
```

Figure III-31: Calculate the volumes in place after history matching

The results are extracted from the PRT file:

III.4.2.3. Comparison between History and Simulator Results:

After many runs and many parameters were varied in order to achieve a Match, we get these optimum results:

The graphs below show the modelled and observed gas production rate of the field and the tubing head pressure of the three wells (GLN-3, GLN-4, GLN-5):

The field:

Figure III-32: Field Gas production rate

GLN-3:

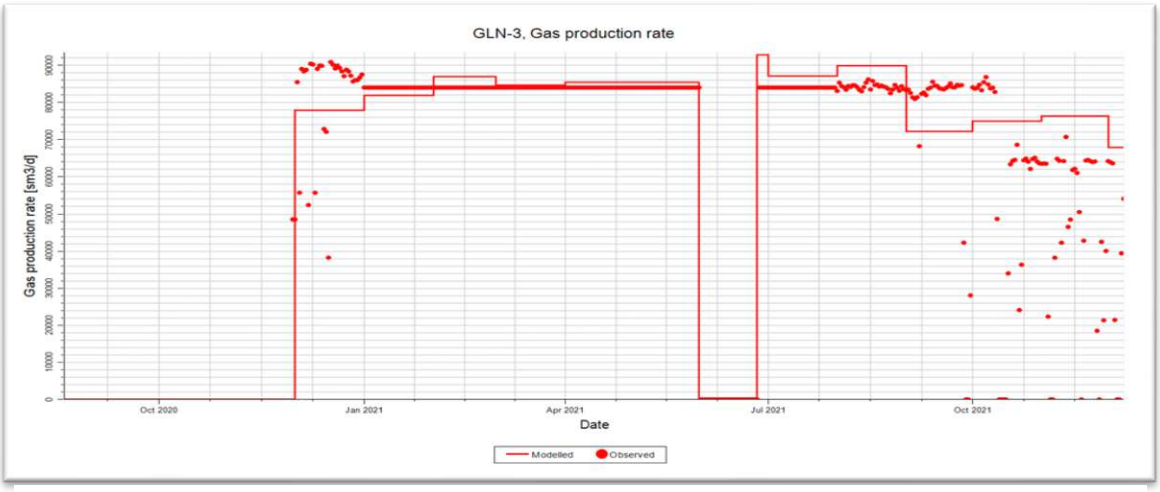

Figure III-34: GLN-3 Gas production rate

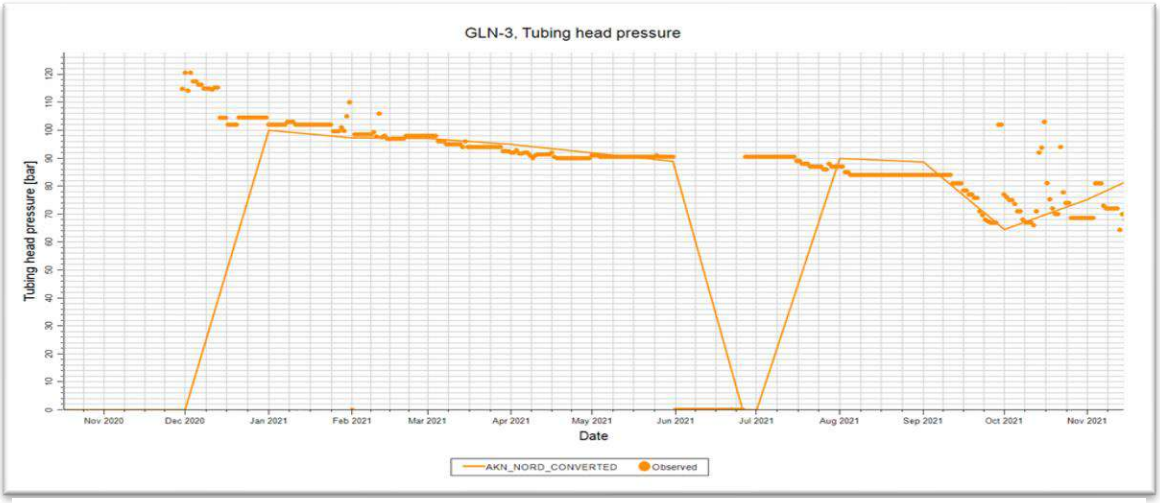

Figure III-33: GLN-3 Gas production rate

GLN-4:

Figure III-35: GLN-4 Gas production rate

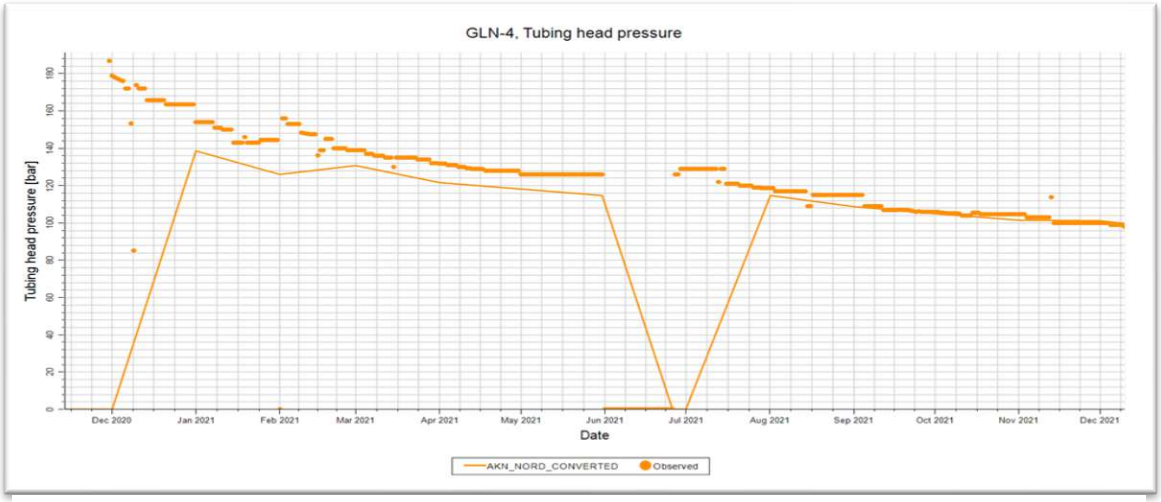

Figure III-38: GLN-4 Tubing Head pressure

GLN-5:

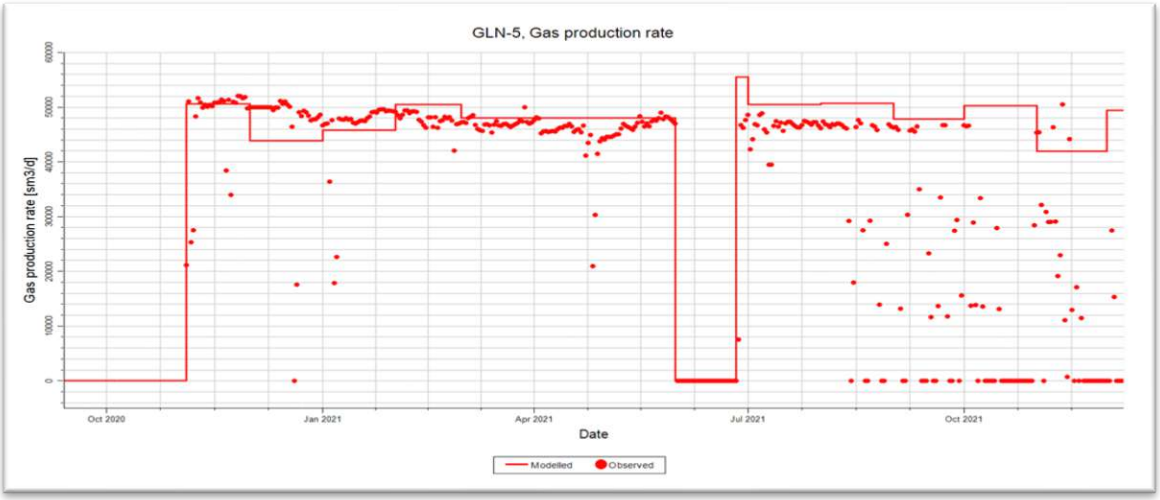

Figure III-37: GLN-5 Gas production rate.

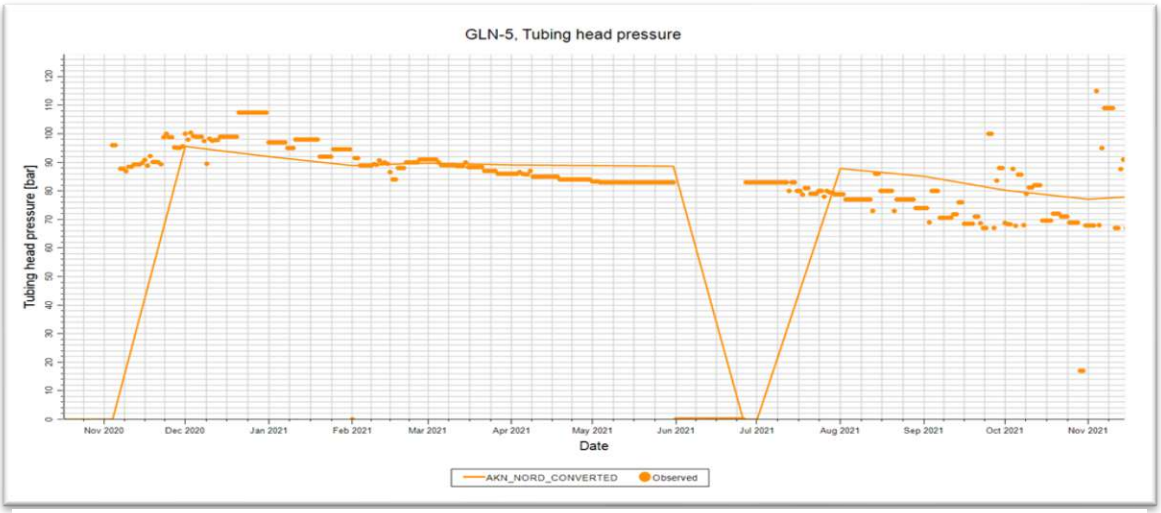

Figure III-36: GLN-5 Tubing head pressure

Description of History Process Used and Parameters Varied:

The following parameters were varied in order to achieve a match:

To match the gas rate more parameters was varied:

- The well transmissibility.
- The perforation local.
- The skin factor.
- The pore volume.

Tables: Summary of Flowing Gas rate History Matching (GLN-3, GLN-4 and GLN-5).

Table III-12 Flowing Gas rate History Matching (GLN-3)

GLN-3					
RUNS	**PI**	**SKIN**	**MULTX**	**MULTPV**	**REMARKS**
1	**6.8**	**1.8**	**-**	**-**	**Too low**
2	**7**	**1.8**	**-**	**-**	**Too low**
3	**7.6**	**1.8**	**-**	**-**	**low**
4	**8**	**2.0**	**-**	**-**	**Slightly low**
5	**9**	**4.5**	**-**	**-**	**Matched**

Table III-13 Flowing Gas rate History Matching (GLN-4)

GLN-4					
RUNS	**PI**	**SKIN**	**MULTX**	**MULTPV**	**REMARKS**
1	**185**	**4.5**	**15**	**1.2**	**Too low**
2	**195**	**4.5**	**20**	**1.4**	**Low**
3	**200**	**4.5**	**26**	**1.5**	**Low**
4	**250**	**3.9**	**28**	**1.9**	**Slightly low**
5	**250**	**3.5**	**30**	**2.0**	**Matched**

Table III-14 Flowing Gas rate History Matching (GLN-5)

GLN-5					
RUNS	**PI**	**SKIN**	**MULTX**	**MULTPV**	**REMARKS**
1	**30**	**12.5**	**-**	**-**	**Too low**
2	**30**	**12.5**	**-**	**-**	**low**
3	**28**	**13.1**	**-**	**-**	**Slightly low**
4	**25**	**14.1**	**-**	**-**	**Matched**

III.5. Predicted Scenarios

Starting from the end of the observed history, the next step was to forecast the performance of the reservoir 50 years into the future with the natural depletion. Deferent scenarios were studied are shown below:

The aggregated production profiles for the GLN study field were constrained by the maximum efficiency rate (MER). The MER is defined in this study as the ratio of the maximum annual production volume to the gross ultimate recoverable volume. Two MER cases (6 and 9 percent) were forecasted for the Best Technical Case to constrain the plateau gas production rate.

III.5.1. Constraints of Simulation Model Forecasts

were the following well constraints applied in GLN field for the forecast cases:

- Minimum well gas production rate: 25,000 cubic meters per day (m^3/d)
- Maximum well water - gas ratio: 0.001 m^3/m^3
- Maximum Well gas production rate: according to DST data
- Minimum wellhead flow pressure: 50 bar Maximum production rates for existing wells were decided based on available DST data.

III.5.2. Scenarios

III.5.2.1. Base case

base case (Production from original production wells) In the first scenario will run the model on fifty years on the future to predict the future performance and the cumulative production of the field by those three wells (GLN-3, GLN-4, GLN-5).

The Results for the base Case are Presented as Followed:

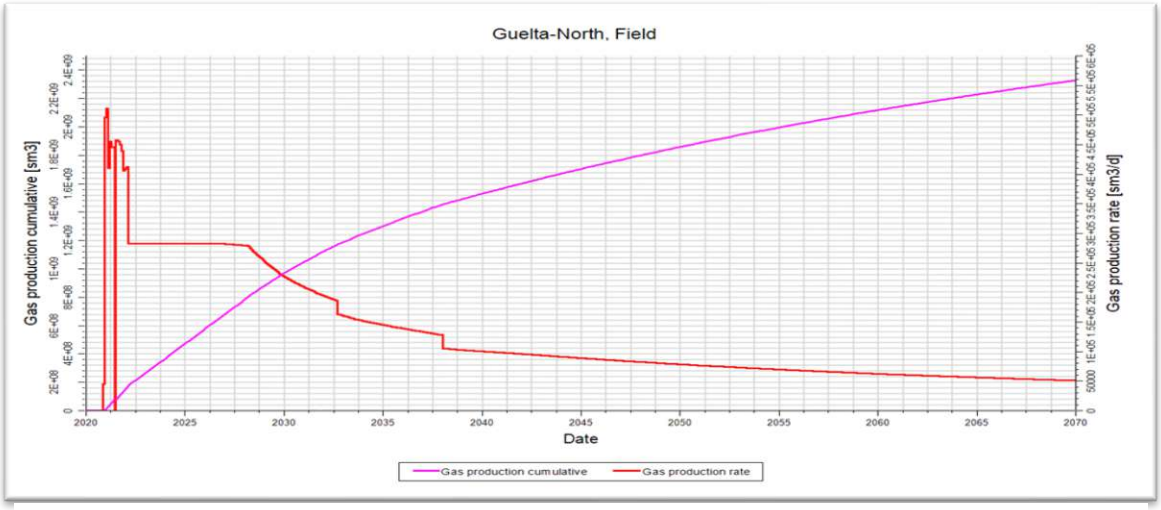

Figure III-39: Guelta north field gas prediction

III.5.2.2. Scenario 1

(MER 6%) add Infill wells (5 additional producing wells added to the gas zone):

In this scenario will add new five producer wells plus the three existing wells (well01, well02, well03, well04, well05).

The Results for The Mer 6 Forecast Case are Presented as Followed:

The Gas Rate and Cumulative Gas Production is shown on figure:

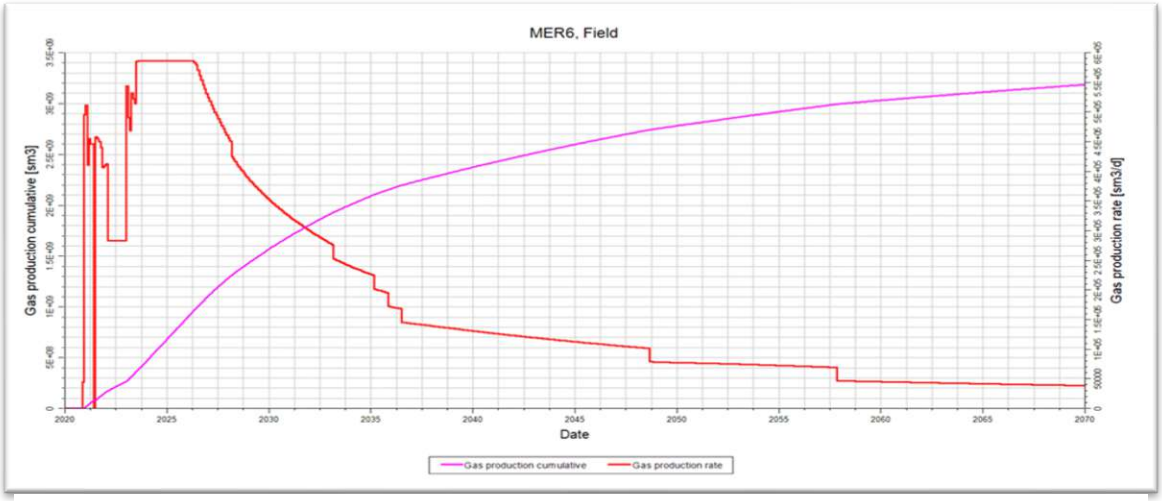

Figure III-40: MER 6 field gas prediction

III.5.2.3. Scenario 2

(MER 9 %) add Infill wells (5 additional producing wells added to the gas zone):

In this scenario will add new five producer wells plus the three existing wells (well01, well02, well03, well04, well05).

The Results for The Mer 9 Forecast Case are Presented as Followed.

The Gas Rate and Cumulative Gas Production is Shown on Figure **Figure III.41:**

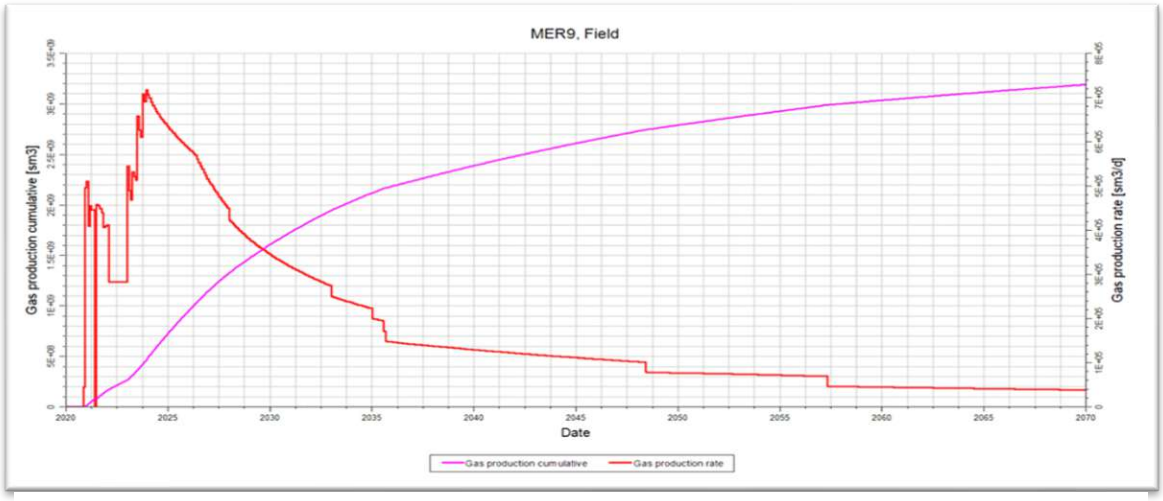

Figure III-41: MER 9 field gas prediction

III.5.2.4. Scenario 3

(Boosting Pressure): create a boosting Pressure station to recording the wells (After drill the infill wells). the following well constraints applied in this scenario are:

- Minimum well gas production rate: 25,000 cubic meters per day (m^3/d)
- Minimum wellhead flow pressure: 20 bar
- Maximum production rates for existing wells were decided based on available DST data.

The Gas Rate and Cumulative Gas Production is Shown on Figure:

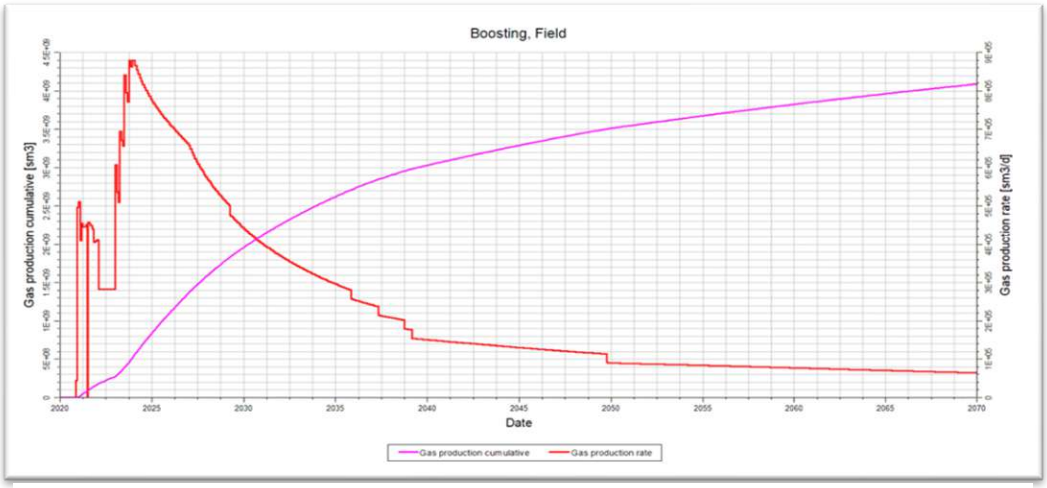

Figure III-42: Gas prediction with boosting pressure scenario

III.5.3. Scenarios results

The table and the graph below show the comparing of the Gas Cumulative for the deferent scenarios after fifteen years of production in the future:

Table III-15 Gas Scenarios results after 50 years

Scenario	Description	Cumulative gas (E+09 Sm3)	Recovery Factor (%)
1	Existing wells	2.33	30.01
2	Infill wells (MER 6%)	3.19	41.10
3	Infill wells (MER 9%)	3.20	41.20
4	Boosting pressure + Infill wells	4.10	52.80

III.5.3.1. Comparison between results:

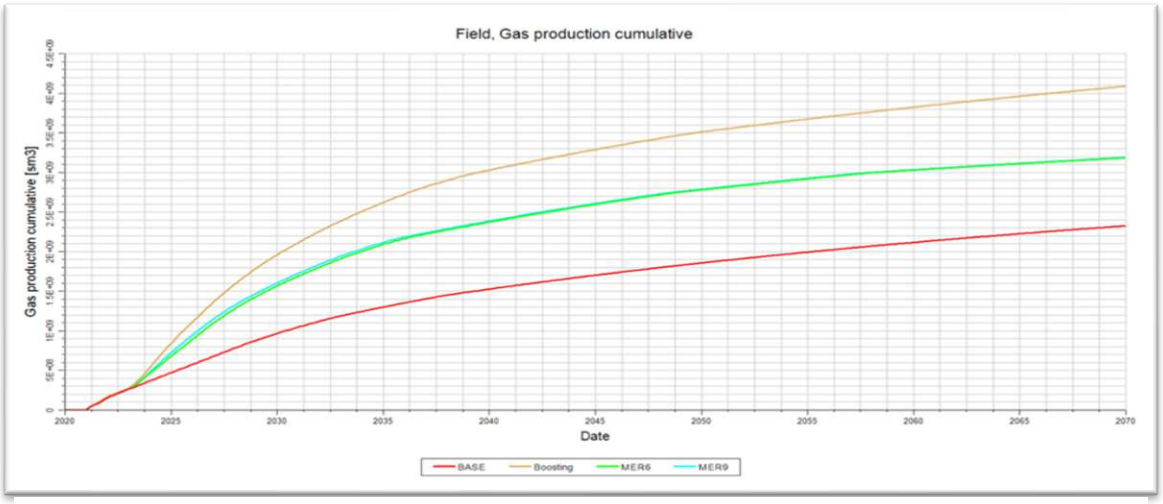

Figure III-43: Compression curve of different scenarios

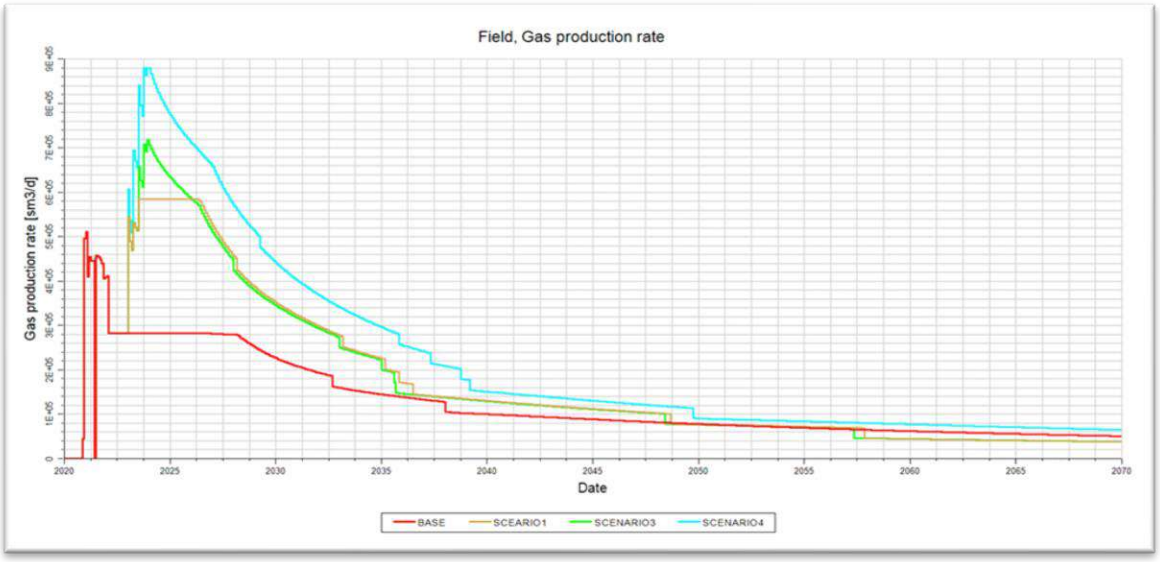

Figure III-44: The four scenarios curve of gas production

III.5.3.2. Discussion of Results

. In the Scenario 1 the results shows that the Field has the capacity to flow at a lower gas production rate. to obtain. The gas recovery from these wells was approximately 30.01%.

. In the Scenarios 2 and 3 the results shows that the Field has the capacity to flow at a higher gas production rate in comparison in Scenario 1. The gas recovery for this scenario was approximately 41.15 %

. In the scenario 4 the results show that the Field have more capacity to flow in comparison in scenarios 2 and 3 at a higher production rate. The gas recovery for this scenario was approximately 52.82%.

After the comparison between the four scenarios, we find that the optimum scenario is the 4^{th} one that has approximately 52.82%.

Remarks

For the forecast simulations, it was considered that one rig would be available for developing the GLN study field and that each well takes 3 months to be drilled and completed. Drilling sequence of the new wells (starting from year 2023) was based on the well cumulative gas recovery estimated from the scoping simulations. New wells were drilled as needed to maintain the constrained production rate (MER) for the GLN study fields. The existing wells come online in January 2021, and the new wells come online starting from 2023 (put date), assuming back-to-back three months drilling and hook up per well.

The new scoping wells are initially completed at the deepest reservoir. When the gas rate drops below a threshold rate, a workover is performed to squeeze the bottom reservoir and open the Upper Reservoir. Additionally, New Wells Were Completed with a Five Meter Standoff Above the GWC To Minimize Water Production.

The ranking of the scenarios is only based on simulation and technical output. Economic analysis of scenarios needs to be conducted and final ranking should be based on net present value and profitability.

Conclusion:

It’s well known that traditional way to improve recovery is drilling a new exploration well, that method has become useless in our modern age in fact of the negative factors has the most chance to be more than positive.

Nowadays In order to efficiently develop and operate a petroleum reservoir, it is important to have a reservoir model. the reservoir numerical simulation model can serve as an appropriate tool for reservoir management to predict the production from each well in a field with multiple wells. The results clearly shows that the gas production has reflected and confirmed to be almost the same result as in real.

with taking the high extraction costs of the Sahara blend (the Algerian crude oil) in old way, it leaves us with only one suitable choice to improve the Algerian recovery factor; to upgrade and develop a dynamic model of the field before the exploration.

Recommandations

☞ The following recommendations provide guidelines for future exploration, appraisal, and development planning considering all available data provided for this study. These include guidelines for data acquisition that may help to reduce the uncertainties identified in this study.

☞ Double check your reservoir data and saturation functions when you are constructing the reservoir model. This part of the project is crucial. If not done properly you would run into a lot of problems matching the provided history data.

☞ It is recommended that future appraisal and development wells in the study area be drilled into the deeper Ordovician reservoirs whenever possible to collect data in these deep reservoirs.

☞ It is recommended that sealed whole cores be obtained for a few wells to accurately estimate porosity, permeability, and water saturation.

☞ To reduce the uncertainty of the core measurements, the core needs to be well preserved.

☞ It is recommended that reservoir engineering data, such as wireline formation pressure and DST data, be collected for as many wells and reservoirs as possible to validate fluid contacts and petrophysical cutoffs.

☞ SCAL measurements are recommended to help establish J function and relative permeability data for rock types with similar pore geometries.

☞ If the objectives of a pressure transient test were not achieved due to operational issues, gas effects, or significant wellbore storage effects, it is recommended that another test in the same well be avoided without eliminating the issues observed in the previous test.

☞ When pressure transient tests, it is recommended that significant flow rate changes be avoided close to a shut - period. If flow rate changes are unavoidable, the flow rate changes should be recorded.

☞ It is recommended that well-test duration be designed so that nearby structural or stratigraphic boundaries can be evaluated. This will yield valuable information on reservoir connectivity in highly faulted areas.

☞ For a pressure buildup test, it is recommended that the total designed test duration be divided between the flowing and shutdown - in periods in such a way as to maximize the amount of usable data obtained from the test. More fluid sample collection and laboratory fluid PVT experiments are recommended to improve understanding of the reservoir fluids. In particular, fluid PVT experiments are highly recommended for the gas - condensate reservoirs. Fluid PVT properties provide valuable information for the purpose of field development planning.

☞ Create a pressure boosting system to increase low pressure in a gas system in order to achieve sufficient gas flow and pressure to the stations.

Bibliography

[1]: Zoltán E. HEINEMANN, fluid flow in porous media, montan universität leoben petroleum engineering department, Leoben, October 2005.

[2]: Guy Barré, Introduction à la simulation numérique des gisements pétroliers, Université de Pau et des Pays de l' Adour (France).

[3]: Reservoir Simulation, Heriot-Watt University.

[4]: Reservoir simulation, Teknica Petroleum Services Ltd. Suite 2500, 530-8th Avenue S.W. Calgary, Alberta T2P 3S8, April 2001

[5]: Tarak Ahmed, RESERVOIR ENGINEERING, HANDBOOK Second Edition, Gulf Publishing Company 2007.

[6]: Raffie Hossein, Advances in petroleum reservoir fluids analysis, Next training 2006.

[7]: Ahmed Tarek 'Reservoir engineering handbook' Gulf Publishing Company 2010.

[8]: What is Reservoir Simulation, eclipse black oil 2017.

[9]: Fanarco, Eclipse 100 user course, Schlumberger.

[10]: Eclipse reference manual 2016, Schlumberger.

[11]: Eclipse-blackoil reservoir simulation, schlumberger ,2007.

[12]: John, R, FANCHI, Principles of applied reservoir simulation, third edition.

[13]: Zhangxin Chen, Calgary, Reservoir Simulation Mathematical Techniques in Oil Recovery Alberta, Canada, 2007. 106

[14]: Kjetil Lorentzen, History Matching a Full Field Reservoir Simulation Model, Norwegian university of science and technology, 2014.

Crude Oil Properties

[15] Cragoe, C.S.: "Thermodynamic Properties of Petroleum Products," U.S. Dept. of Commerce, Washington, DC (1929) 97.

[16] Standing, M.B.: Volumetric and Phase Behavior of Oil Field Hydrocarbon Systems, SPE, Richardson, TX (1977) 124.

[17] Vazquez, M. and Beggs, H.D.: "Correlations for Fluid Physical Property Prediction," JPT (June 1980) 968-70.

[18] McCain, W.D. Jr., Rollins, J.B., and Villena, A.J.: "The Coefficient of Isothermal Compressibility of Black Oils at Pressures Below the Bubblepoint," SPEFE (Sept. 1988) 659-62; Trans., AIME, 285. 10.

[19] W.D. McCain.Jr. "Reservoir Fluid Property Correlations-State of the Art," SPE Reservoir Engineering, (May 1991) p. 266.

Natural Gas Properties

[20] Standing, M.B. and Katz, D.L.: "Density of Natural Gases," Trans., AIME (1942) 146, 140-49.

[21] Dranchuk, P.M. and Abou-Kassem, J.H.: "Calculations of z-Factors for Natural Gases Using Equations of State," J. Cdn. Pet. Tech. (July-Sept. 1975) 34-36.

[22] Lee, A.L., Gonzalez, M.H., and Eakin, B.E.: "The Viscosity of Natural Gases," JPT (Aug. 1966) 997-1000; Trans., AIME (1966) 234.

Inflow performance modeling

[23] Rawlins, E.L. and Schellhardt, M.A. 1935. Backpressure Data on Natural Gas Wells and Their Application to Production Practices, 7. Monograph Series, U.S. Bureau of Mines.

[24] SONATRACH/IAP-CU, MSC.SIMOHAMED Elyazid, Inflow Performance Modelling & Well Testing.

[25] Omar Falih Al-Fatlawi.” Numerical Simulation for the Reserve Estimation and Production Optimization from Tight Gas Reservoirs. December 2018.P23-33.

[26] https://www.software.slb.com/products/eclipse.